

2006

Microscopy of the turtle utricle and its innervation

Heeral C. Kothari
San Jose State University

Follow this and additional works at: https://scholarworks.sjsu.edu/etd_theses

Recommended Citation

Kothari, Heeral C., "Microscopy of the turtle utricle and its innervation" (2006). *Master's Theses*. 2898.
DOI: <https://doi.org/10.31979/etd.z2re-mwe9>
https://scholarworks.sjsu.edu/etd_theses/2898

This Thesis is brought to you for free and open access by the Master's Theses and Graduate Research at SJSU ScholarWorks. It has been accepted for inclusion in Master's Theses by an authorized administrator of SJSU ScholarWorks. For more information, please contact scholarworks@sjsu.edu.

MICROSCOPY OF THE TURTLE UTRICLE AND ITS INNERVATION

A Thesis

Presented to

The Faculty of the Department of Biological Sciences

San José State University

In Partial Fulfillment

of the Requirements for the Degree

Master of Science

by

Heeral C. Kothari

May 2006

UMI Number: 1436924

INFORMATION TO USERS

The quality of this reproduction is dependent upon the quality of the copy submitted. Broken or indistinct print, colored or poor quality illustrations and photographs, print bleed-through, substandard margins, and improper alignment can adversely affect reproduction.

In the unlikely event that the author did not send a complete manuscript and there are missing pages, these will be noted. Also, if unauthorized copyright material had to be removed, a note will indicate the deletion.

UMI[®]

UMI Microform 1436924

Copyright 2006 by ProQuest Information and Learning Company.

All rights reserved. This microform edition is protected against unauthorized copying under Title 17, United States Code.

ProQuest Information and Learning Company
300 North Zeeb Road
P.O. Box 1346
Ann Arbor, MI 48106-1346

© 2006

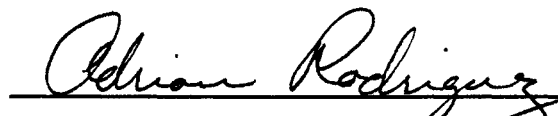
Heeral C. Kothari

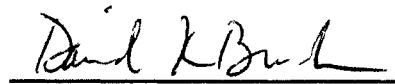
ALL RIGHTS RESERVED

MICROSCOPY OF THE TURTLE UTRICLE AND ITS INNERVATION


APPROVED FOR THE DEPARTMENT OF BIOLOGICAL SCIENCES

 Biol. Sci. 3/16/06
Dr. Michael Sneary (Chair) Department Affiliation Date

 Biological Sciences 3/16/06
Dr. Adrian Rodriguez Department Affiliation Date

 Biological Sciences 3/16/06
Dr. David Bruck Department Affiliation Date

APPROVED FOR SAN JOSÉ STATE UNIVERSITY

 03/25/06
Date

ABSTRACT

MICROSCOPY OF THE TURTLE UTRICLE AND ITS INNERVATION

By Heeral C Kothari

The present study expands the database of structural information for the reptilian utricle. Light microscopy (LM), scanning electron microscopy (SEM), and transmission electron microscopy (TEM) were used to study the utricle of the red-eared slider turtle, *Trachemys scripta elegans*. This study provides the first SEM images of the reptilian gelatinous membrane (a component of the overlying inertial mass) and additional details concerning the structure of hair cell kinocilia. TEM images of supporting cells, hair cells, connections between stereocilia, and nerve fibers are presented for the first time. Information derived from sections taken in three specimens at several locations was used to calculate the total number of nerve fibers (afferent and efferent) in the utricular nerve. From this, a hair cell/nerve fiber ratio was calculated. Finally, a sample of the range of nerve fiber diameters is presented.

ACKNOWLEDGEMENTS

This study was conducted at the neurosensory laboratory of Dr. Michael Sneary at San José State University. I would like to thank Dr. Sneary for his unwavering support and guidance throughout my graduate career at San José State University. His assistance and encouragement have contributed in making this research and manuscript possible. My appreciation also goes out to Dr. David Bruck, whose course on transmission electron microscopy helped me effectively use the technique during my research. This manuscript would have not been complete without the expert comments and suggestions by Dr. Adrian Rodriguez and Dr. Bruck.

I would also like to thank Melissa Carter, formerly at the Microscope and Graphics Imaging Center (“MAGIC”) at California State University, East Bay, and Anastasia Micheals at the Materials Characterization and Metrology Center, San José State University. Without their direction and expertise, the scanning electron micrographs would not have been possible. I would also like to thank Marco (Optics Maintenance) and Ron (Computer and Instrumentation Support Center) for their support.

My deepest gratitude goes to my parents for their constant encouragement and love, in-laws for their support, and friends for always being there. Lastly, my husband, Chetan, deserves many thanks for his encouragement, patience, and love.

TABLE OF CONTENTS

INTRODUCTION	1
Overview of the Vestibular System	1
Anatomy of the Utricle	2
Comparison of the Utricle in Different Species.....	5
Mammals.....	5
Birds	6
Fish.....	7
Amphibians	8
Reptiles	9
Vestibular Nerve	11
Present Study	15
MATERIALS AND METHODS.....	17
Light Microscopy.....	18
Transmission Electron Microscopy	19
Scanning Electron Microscopy	19
RESULTS	21
Gross Morphology of the Inner Ear	21
The Macular Surface of the Utricle (Scanning Electron Microscopy)	21
Striolar Bundles	22
Extrastriolar Bundles	22

Light Microscopy and Transmission Electron Microscopy of the Macula	23
Supporting Cells.....	23
Hair Cells	24
Vestibular Nerve	25
DISCUSSION	27
Utricular Macula	27
Surface and Hair Bundle Morphology	27
Epithelial Ultrastructure	29
Vestibular Nerve	31
Gross Anatomy	31
Light Microscopy and Transmission Electron Microscopy	31
Future Directions	34
BIBLIOGRAPHY	35
APPENDIX 1: FIGURES AND TABLES	38
LIST OF FIGURES	39
FIGURE 1. Schematic cross-sectional diagram of the utricle	A-1
FIGURE 2. Diagram of the utricular macular hair cell populations.....	A-2
FIGURE 3. Macular shape and hair bundle orientation patterns of various species	A-3
FIGURE 4. Relative position of the inner ear.....	A-4
FIGURE 5. SEM of the utricle and semicircular cristae surfaces	A-5
FIGURE 6. SEM of the macula and overlying layers	A-6
FIGURE 7. SEM of the otoconial layer.....	A-7

FIGURE 8a. SEM of the surface of the utricle.....	A-8
FIGURE 8b. A tracing of the utricular macular surface.....	A-8
FIGURE 9. SEM of the attachment of a hair bundle to the overlying membrane.....	A-9
FIGURE 10a. SEM of striolar hair bundles.....	A-10
FIGURE 10b. SEM of juxtastriolar hair bundles.....	A-11
FIGURE 11a. SEM of rampary hair bundles.....	A-12
FIGURE 11b. SEM of rampary hair bundle	A-13
FIGURE 12. SEM of cotillary hair bundles.....	A-14
FIGURE 13. LM of a coronal section of the macula and surrounding tissues	A-15
FIGURE 14. TEM of supporting cells.....	A-16
FIGURE 15. TEM of transverse section of a hair bundle.....	A-17
FIGURE 16. TEM of a hair cell and surrounding supporting cells.....	A-18
FIGURE 17. TEM of an afferent synaptic body.....	A-19
FIGURE 18. TEM of a cellular process beneath the hair cell	A-20
FIGURE 19. LM and tracing of inner ear pars superior	A-21
FIGURE 20. LM of the epithelium.....	A-22
FIGURE 21. LM of a myelinated fiber within the epithelium	A-23
FIGURE 22. TEM of a nerve fiber gaining myelin.....	A-24
FIGURE 23. TEM of myelinated nerve fiber and extracellular material	A-25
FIGURE 24. TEM of a myelinated axon.....	A-26
FIGURE 25. LM of the anterior ganglion	A-27
FIGURE 26. LM of the anterior ganglion cells.....	A-28

FIGURE 27. TEM montage of two ganglion cells	A-29
FIGURE 28. TEM of capillary and RBC.....	A-30
FIGURE 29. TEM of a mast cell	A-31
FIGURE 30a. LM of the anterior branch of the eighth nerve.....	A-32
FIGURE 30b. LM of the eighth nerve	A-33
LIST OF TABLES	73
TABLE 1. Stereocilial counts in hair bundles of different regions of the macula.....	A-34
TABLE 2. Comparison of the average number of stereocilia per bundle	A-34
TABLE 3. Nerve fiber averages from three individual specimens.....	A-35
TABLE 4. Average diameters of nerve fibers	A-35
APPENDIX 2: SOLUTION FORMULATIONS	76

INTRODUCTION

Overview of the Vestibular System

The vertebrate inner ear includes two highly specialized sensory systems. The auditory system detects sound waves. Abnormal development or malfunctions of this system may lead to problems in sound identification and localization and ultimately to deafness. The vestibular system has three functions: (a) detection of angular accelerations, (b) detection of linear accelerations, and (c) detection of substrate-borne (seismic) vibrations. Information derived from the above sensors may be used to maintain and regulate the tonus of the body musculature and to control the position of the eyes with respect to the head (Sondag, 1996).

There are two types of vestibular end organs in the inner ear that are specialized to detect either angular (semicircular ducts) or linear acceleration (utricle, saccule, and lagena) of the head. The three semicircular ducts house a sensory epithelium (crista) in each of their ampullae (expanded end of each semicircular duct). The structure and function of the semicircular ducts are highly conserved across the vertebrate taxa. In contrast, the saccule and lagena have a variety of functions ranging from auditory to vestibular to seismic. The lagena is found in cartilaginous fish, birds, and mammals (monotremes only). In the bluegill (fish) and newts (amphibians), the function of the lagena is to detect sound waves, whereas in frogs (amphibians), turtles (reptiles), and chicks (birds) the function is maintenance of equilibrium (Harada et al., 2001). The utricle has a consistent function of detection of linear acceleration in terrestrial

vertebrates. In contrast, in the sleeper goby (a fish), the utricle has both vestibular and auditory functions (Lu et al., 2004).

Anatomy of the Utricle

The utricle is a fluid-filled, sac-like structure located ventral to and between the ampullae of the anterior and lateral semicircular ducts. It is in anatomic continuation with these ampullae dorsally and with the saccule ventrally. The utricle is part of the membranous labyrinth and is filled with endolymphatic fluid. This fluid is high in potassium and low in sodium and calcium (similar to intracellular fluid) and plays an important role in mechanotransduction (Colclasure and Holt, 2003). A layer of epithelial cells lines the utricular space. This layer is specialized in one area to form a sensory epithelium (macula) positioned approximately in the horizontal plane of the head.

A trans sectional view of the utricle reveals the presence of three sequential layers from top to bottom: an inertial mass, the gelatinous membrane, and the sensory epithelium (Ladich and Popper, 2001) (Figure 1). The utricular macula in fish is covered with an inertial mass in the form of a single stone called an otolith. In mammals, reptiles, amphibians, and birds, it is covered with a particulate (or otoconial) mass. This mass is made up of thousands of otoconia (ear sand) averaging 10 μm in length (Lins et al., 2000). The inertial mass increases the sensitivity of the macula to linear accelerations.

Otoconia consist of microcrystals joined together by an organic matrix to form composite crystals. Calcium carbonate crystals form the mineral phase of most otoconia but exceptions exist (Lins et al., 2000). The most common calcium carbonate found in

fish is aragonite. However, calcite, vaterite, and calcium carbonate monohydrate are also present. The otoconia in amphibian utricles are calcite polymorphs (Kido and Takahashi, 1997) and usually have a barrel-like body terminated by three facets at both ends (Steyger and Wiederhold, 1995; Lychakov, 2004).

Beneath the inertial mass is the gelatinous membrane. This membrane consists of two structurally distinct layers: a peripheral layer and a subcupular (so called in mammals) layer. The peripheral layer supports the overlying otoconia. The subcupular layer extends down to the surface of the sensory epithelium (Takumida et al., 1992). The gelatinous membrane surrounds hair bundles projecting from the surface of hair cells. Each bundle consists of many short “hairs,” the stereocilia (microvilli), arranged according to height, and one long “hair,” the kinocilium. The diameter of each stereocilium is smaller at its base, while that of the kinocilium does not change. The longer stereocilia are located near the kinocilium so that the entire bundle takes on an “organ pipe” configuration. The kinocilium and some of the longer stereocilia may be attached to the overlying gelatinous membrane. In addition, the kinocilium is attached to the longer stereocilia, and there are interstereociliary connections called “tip-links.” These links run from the tips of the shorter stereocilia to the sides of the longer stereocilia in the next highest row (Sondag, 1996). Adjacent stereocilia are attached to one another by side links and ankle links at the beginning of the taper (Frolenkov et al., 2004). Linear acceleration of the head results in an inertial displacement of the mass above the epithelium. This causes the attached kinocilium (and longer stereocilia) to bend. Due to the various attachments, the result is deflection of the entire bundle. Deflection of the

bundle towards the kinocilium results in an influx of cations through the tips of the stereocilia and depolarization of the hair cell. This leads to an increase in the frequency of action potentials in the vestibular afferent neurons. Deflection of the bundle away from the kinocilium results in a decrease in action potential frequency in the afferent neurons (Sondag, 1996; Colclasure, 2003). These bundles therefore display structural and functional polarity. The hair cell population of the utricular macula is divided into two regions. Each population is oriented towards an imaginary line of polarity reversal that is usually present in the striolar region. Hair bundles on either side of this line are oriented opposite to each other. The exact location of this line of polarity reversal varies from species to species.

The shape of the utricular macula also differs from species to species, and its surface is generally differentiated into three regions: rampa, striola, and cotillus. Each region is characterized by different hair bundle morphologies (Figure 2). In general, the striolar region runs the entire length of the macula, and is characterized by hair cells each having a bundle consisting of numerous stereocilia and a single kinocilium not much longer than the tallest stereocilium. The kinocilia in the striolar region are characterized by a prominent “bulb” (expanded end of the kinocilium) at their tips. The striola separates the rampa and cotillus (both sometimes designated as extrastriola); the rampa is present laterally and the cotillus medially. These regions are characterized by hair cells each having a bundle consisting of fewer stereocilia and a longer kinocilium.

There are two types of hair cells present in the neuroepithelium. Type I hair cells are amphora-shaped (have a rounded bottom with a narrow neck). Type II hair cells are

cylindrical (Figure 1). Type I hair cells are innervated by afferent nerve fibers ending in calyceal terminals that engulf the cells, whereas type II hair cells are innervated by bouton afferent terminals (Figure 1). Dimorphic afferents contact both types of hair cells. A dimorphic afferent ending on a type I hair cell has a calyceal terminal, whereas on type II hair cells it has bouton terminals. The relative proportions of these afferent nerve fiber terminals differ from one species to another. The sensory epithelium also contains supporting cells whose numbers are far greater than those of the hair cells (Figure 1). Supporting cells usually span the entire height of the epithelium. The apical surface of each of these cells has numerous microvilli and a single, central, short, ciliary rod (Kirkegaard and Jorgensen, 2001). Also present in the epithelium are efferent nerve fibers. They are much smaller in diameter than afferents and branch extensively (Si et al., 2003).

Comparison of the Utricle in Different Species

Mammals

In mammals, the utricle is heart-shaped (Figure 3) (Sondag, 1996). There is a narrow striola that runs the entire length of the neuroepithelium and separates it into two broader extrastriolar regions (Figure 3). The striola in the mouse, rat, gerbil, guinea pig, chinchilla, and tree squirrel is a C-shaped region (Desai et al., 2004). The otoconia over the striola are small compared to those in the extrastriolar regions. The hair cells of the striolar region are less densely packed and have shorter hair bundles with more stereocilia compared to hair bundles in the extrastriola. The striola consists of type I and type II hair

cells. Here, type I hair cells outnumber type II hair cells. The line of polarity reversal in mammalian utricles runs through the middle of the striola. On either side of the striola lies a juxtastricular region with a mixture of type I and type II hair cells. In the extrastricular regions, the two types of hair cells occur in nearly equal numbers. The hair bundles in the extrastricular regions are oriented towards the striola and, thus, the line of polarity reversal separates a population of oppositely polarized hair cells (Desai et al., 2004).

Birds

The surface of the utricular macula in the pigeon is rectangular with a rounded anterior edge (Figure 3). The posterior edge of the macula is strongly indented so that the epithelium has a prominent tail region (Si et al., 2003). The striola is located near the lateral border of the macula (Figure 3). In birds, the striola is distinct from other species. There is a narrow band of type II hair cells, six-to-eight hair cells in width, known as the “Type II Band.” The type II band runs through the middle of the striola, and the line of polarity reversal runs through this band of type II hair cells. On either side of the type II band are zones of mixed type I and type II hair cells (Si et al., 2003). The line of polarity reversal runs through the entire macula. The polarization of hair cells along the line of reversal follows two different morphological patterns in the pigeon. Hair cells in the lateral and anterior regions have bundles directed towards the reversal line, whereas hair bundles in the medial macula are parallel to the reversal line, with bundles on either side of the reversal line being anti-parallel to each other (Figure 3) (Si et al., 2003).

The striolar region consists of three separate zones: the medial striolar zone, lateral striolar zone, and the type II band. The medial and lateral striolar zones are rich in type I hair cells, whereas the type II band is rich in type II hair cells. Outside the striola is the extrastriolar region that consists entirely of type II hair cells.

Fish

In teleost fish, the utricular macula is almost round with a finger-like projection (lacinia), a lateral extension of the anterior margin (Ladich and Popper, 2001)(Figure 3). Two types of hair cell ciliary bundles are found in the utricular macula, type F1 and F2. F1 ciliary bundles bear short stereocilia and a kinocilium no longer than twice the length of the tallest stereocilium. Type F2 bundles also bear short stereocilia but with kinocilia heights more than three times the height of the tallest stereocilia. The distribution of hair cells in the fish utricle is as follows: the cells along the narrow anterior border have bundles oriented medially, whereas the ciliary bundles of the large central group are oriented laterally (Figure 3). This pattern is also found in the lacinia. The actual transition occurs in the striola. F1 hair cell bundles are found in the central region of the striola and in the extrastriolar region. F2 ciliary bundles are found at the margins of the striola and within the lacinia (Ladich and Popper, 2001).

In the lungfish (Protopterus), the utricle is very large in size compared to other species. It contains a flattened bowl-shaped macula having a striola and extrastriolar cotillus. A clear lateral or caudal extension of the macula has not been observed in this species. The

calcified otolith masses found in the other teleost fish are absent in the lungfish. Instead, the otoconial mass is paste-like within a gelatinous matrix (Platt et al., 2004).

The striola is located along the lateral edge of the macula and contains two oppositely oriented groups of hair cells. There is no rampa. The striolar hair cells along the outer edge of the epithelium are oriented towards the line of polarity reversal opposing the group of hair cells from the medial side. The extrastriolar region consists of the medially located cotillus. The cotillus contains a sparse population of hair cells with bundles of fewer stereocilia than those in the striola. The hair cells in the cotillus are oriented towards the striola.

Amphibians

The utricular macula in the bullfrog is a kidney-shaped structure. It possesses only type II hair cells with distinctive hair bundle morphologies, and is divided into large medial and smaller lateral extrastriolar regions by the striola (Figure 3) (Baird and Schuff, 1994). The hair cells in the striola tend to be larger and are more widely spaced than those in either of the extrastriolar regions. The line of polarity reversal is located near the lateral border of the striola, separating the striola into medial and lateral rows. On average, the striola consists of 5-7 medial rows and 2-3 lateral rows of hair cells (Baird, 1994). Different types of hair cells are found in each of the medial and lateral striolar rows. Type E cells have smaller hair bundles and prominent kinociliary bulbs. These cells are found only in the innermost striolar rows on both sides of the line of polarity reversal. Type F cells are confined to the middle striolar rows. They have hair

bundles with stereocilia numbers greater than other utricular hair cell bundles and kinocilia equal or slightly longer than the longest stereocilia in the bundle. Type C cells bear stereocilia and kinocilia that are approximately twice as long as those of type B cells. These cells are confined to the striola and are more numerous in the outer striolar rows. The hair cells in either of the extrastriolar regions are oriented towards the striola, and hair cells in the striola are oriented in the same direction as the adjacent extrastriolar hair cells. The extrastriolar regions have type B cells. They have a small apical surface and short stereocilia. The kinocilia of these cells are 2-6 times longer than the longest stereocilia present in the bundle. Type B cells are the predominant hair cell type in the utricular macula and are found throughout the cotillus and rampa and more rarely in the striola (Baird, 1994).

Reptiles

In turtles, the utricle lies ventrally between the anterior and lateral ampullae and is slightly concave (Figure 3) (Fontilla and Peterson, 2000). The striola extends from the anterior to the posterior edge of the macula (Figure 3). It bears both type I and type II hair cells. Both the anterior and posterior parts of the striola are very narrow, and consist of only one or two hair cells (Severinsen et al., 2003). The border between the striola and rampa corresponds approximately to the line of hair cell polarity reversal (Fontilla and Peterson, 2000). The rampa and cotillus bear only type II hair cells. The hair cells in these two extrastriolar regions are oriented towards the striola. Within the striola, hair cells are also oriented towards the line of polarity reversal. Light microscopic studies

indicate the following distribution of hair cell types. Type I hair cells are found exclusively in the striola in reptiles (Severinsen, 2003; Si et al., 2003). Type II hair cells occur throughout the macula.

Severinsen et al. (2003), reported striolar type I and II hair cells as having large elevated apical surfaces that are oval to ovoid in shape. The stereocilia in each bundle are arranged in 8-10 rows with 5-12 stereocilia in each row (average of 67 stereocilia per bundle). The kinocilium in each hair bundle is 5-7 μm long. Cotillary hair cells have stereocilia arranged in 7-12 rows with 4-6 stereocilia in each row (average of 44 stereocilia per bundle). The kinocilium in these bundles is 7-13 μm long. Rampary hair cells have bundles with stereocilia arranged in 6-10 rows with 5-7 stereocilia in each row (average of 38 per bundle). Each rampary hair bundle has a kinocilium approximately 8-11 μm long (Severinsen et al., 2003). Moravec and Peterson (2004) observed striolar type I hair bundles with significantly more stereocilia (average of 96 per bundle) than striolar type II hair bundles (average of 60). Furthermore, in that study, striolar type II hair bundles had significantly more stereocilia per bundle than adjacent rampary (42 per bundle) and cotillary (average of 54 per bundle) type II hair bundles. The difference in numbers of stereocilia obtained in the two studies may be due to the different methods employed to obtain the counts. One study derived an estimate of numbers from a sampling technique (Severinsen et al., 2003), whereas the other study derived stereocilia numbers from optical sections through the base of the bundles (Moravec and Peterson, 2004).

A study of heights of kinocilia by means of differential interference contrast (DIC) microscopy showed that the height varies across the surface of the macula (Fontilla and Peterson, 2000). However, there is an abrupt change in kinocilial heights from short to long that is coincident with the line of polarity reversal near the lateral edge of the striola (Fontilla and Peterson, 2000). In addition, the height variation in the kinocilia is not tied to hair cell type as both the cotillus and rampa contain only type II hair cells. Rampary kinocilia are longer than those in the cotillus. Striolar cells have short kinocilia in both type I and type II hair cells (Fontilla and Peterson, 2000).

Vestibular Nerve

The vertebrate eighth cranial nerve supplies both auditory and vestibular sensors. The posterior branch of the nerve supplies part of the saccular macula, posterior crista, papilla neglecta, lagenar macula, and the basilar papilla. The anterior branch supplies the anterior and lateral semicircular cristae, remainder of the saccular macula, and the utricular macula (Sneary, 1988).

Leake (1974) provided a detailed description of the anterior branch of the eighth nerve and its innervation pattern in the reptile, *Caiman crocodilus* (South American alligator or spectacled caiman). Leake considers the anterior ganglion to be functionally homologous to the Scarpa's Ganglion in mammals. It contains the cell bodies of afferent nerve fibers innervating the anterior and lateral cristae, most of the saccule, and the utricle. In *crocodilus*, the nerves from the anterior and lateral cristae fuse just ventral to their respective ampullae. Most anterior ganglion cells are found ventral to this point of

fusion. At about the same level, fibers from the utricular macula join the nerve medially. The ganglion cells for the utricular nerve fibers are positioned medially too. The last nerve to make a large contribution to the anterior ganglion is the saccular nerve. The fibers then pass from the anterior ganglion as the anterior branch of the eighth nerve, and enter the brain stem ventral and slightly rostral to the posterior branch of the eighth nerve (Leake, 1974). In the monitor lizard (*Varanus exanthematicus*), cell bodies of the efferent nerve fibers are located between the abducens nucleus and superior olive in the brain, and send their peripheral processes out into the anterior and posterior branches (Barbas-Henry and Lohman, 1988). In most cases, the axons of afferent and efferent fibers enter the neuroepithelium and branch to innervate more than one hair cell (Si et al., 2003). Physiological diversity in afferents is associated with the morphology and spatial location of afferent terminals in the neuroepithelium. For instance, type I hair cells with calyceal afferent terminals and type II hair cells with bouton terminals may have distinctive properties that contribute to functional diversity in their postsynaptic afferents (Xue and Peterson, 2006). Bundle heights affect bundle mechanics and hair cell transduction. Hence, Xue and Peterson suggested that location- and type-specific differences in bundle heights contribute to differences in bundle mechanics, hair cell transduction, and ultimately, afferent responses to head movement.

In the bullfrog, afferent nerve fibers terminate only in non-calyceal terminals (Baird and Schuff, 1994). Most of these endings are en passant or terminal bouton-like endings. The striolar afferents in bullfrogs have thick axons, larger terminal fields, more synaptic endings, and innervate larger number of hair cells. Many of these afferents have club-

like or claw-like synaptic specializations at the end of relatively thick branches of the parent axon. These endings do not completely surround the basolateral surface of hair cells and are always associated with bouton-like endings (found on thinner branches). Juxtastricular afferents are similar to stricular afferents in that they have few subepithelial bifurcations, large terminal fields, and contact many hair cells. However, unlike stricular afferents, they have thin parent axons, lack specialized synaptic endings, and possess fewer synaptic endings per hair cell. These characteristics of juxtastricular afferents are similar to those of the medial extrastriola. One unique characteristic of juxtastricular afferents is that they enter the sensory epithelium and travel for long distances without making contacts with hair cells. The morphology of the lateral extrastriolar afferents is similar to those in the juxtastricola. Hence, in the bullfrog, juxtastricular afferents have morphologies transitional between medial extrastriolar and stricular regions. Afferents destined for the medial extrastriola seldom bifurcate below the sensory epithelium and, if so, contact closely adjacent groups of hair cells.

Due to the specific location of different hair cell types in the macula, the extrastriolar and juxtastricular afferents exclusively innervate type B hair cells. On the other hand, afferents innervating the striola innervate a complex mixture of hair cells. Afferents supplying the outer rows of the striola innervate a large number of type B and type C hair cells. Those innervating the more central stricular rows contact a complex mixture of the four hair cell types. A small number of stricular afferents, with thin parent axons, supply only the innermost rows of the striola, contacting relatively large numbers of type E and type F hair cells (Baird and Schuff, 1994).

In the pigeon, calyceal afferents are found exclusively in the striolar region, and the size and structure of the calyx terminals varies widely (Si et al., 2003). Calyceal terminals can contain as many as 6 type I hair cells. Structurally, two profiles are observed: a globular or “flower-shaped” profile of calyceal terminals that contain hair cells in close approximation, and a thin rectangular-shaped profile that contains a linear array of hair cells (Si et al., 2003). A few of these calyceal afferents have also been observed to make bouton contacts with nearby hair cells. These dimorphic afferents in the pigeon are located predominantly in the striolar region. A few dimorphs have been observed outside of the striola (Si et al., 2003). These fibers innervate a number of type II hair cells and then continue to the striolar region, where calyceal terminals are developed. Several of the dimorphic afferents innervate the type II band region in the striola. Flower and linear profiles have also been observed in the dimorphs.

Bouton terminals are found exclusively on type II hair cells and are located in the extrastriolar regions and in the type II band (Si et al., 2003). Flower and linear profiles are also observed for fibers making bouton terminals. Flower profiles consist of radiating branching patterns extending from the parent axon as it enters the epithelium, whereas linear profiles consist of branching patterns extending along a narrow width of the macular surface (Si et al., 2003).

In birds, cell bodies of vestibular efferents are in the brain stem ventral and slightly lateral to the abducens nucleus. Innervation patterns of efferent fibers are distinctive from afferent fibers as can be visualized in BDA- (Biotinylated Dextran Amine) stained specimens. Efferent fibers branch several times beneath the neuroepithelium and have

thin parent axons. The efferent parent axons extend for several hundred μm , and then fine branch fibers extend into the epithelium. These branches display a high density of en passant and terminal boutons (Si et al., 2003). The efferent terminals are smaller than the afferent bouton terminals.

Present Study

In the present study, the utricular macula of the red-eared slider turtle, *Trachemys scripta elegans*, was investigated using the techniques of scanning electron microscopy (SEM), transmission electron microscopy (TEM), and light microscopy (LM). This study extends those described above and provides further insight into comparative and evolutionary relationships. The turtle inner ear has been a model system for vertebrate auditory function for several decades (Jorgensen, 1974; Sneary, 1988). In the same manner, the functional and structural organization of the turtle utricular macula is similar to that found in mammals and, hence, can be used to understand general functional as well as dysfunctional parameters.

Specifically, this study adds to the database of the ultrastructural features of the reptilian utricular macula. TEM images of supporting cells, hair cells, and connections between the stereocilia in utricular hair bundles are presented for the first time. SEM images of the gelatinous membrane and the unique morphology of striolar and juxtastriolar kinocilia were also observed and reported. Furthermore, a report of the total number of nerve fibers (afferents and efferents) in the anterior branch of the vestibular nerve is provided along with an estimate of the number of nerve fibers supplying the

turtle utricular macula. The present study also reports the ultrastructure of the anterior eighth nerve and ganglion. Nerve fiber diameters of the reptilian anterior eighth nerve are reported. In addition, hair cell to nerve fiber ratio is reported for the first time.

MATERIALS AND METHODS

Five red-eared slider turtles, *Trachemys scripta elegans*, were used in the present study. All animals were adult in size and ranged from 480 to 785 g in weight. During handling of the animals, San Jose State University Animal Care and Use Committee guidelines were followed at all times (Protocol #650).

The turtles were anesthetized by intramuscular injection of 100 mg per kg body weight of Ketaset® (ketamine hydrochloride injection, USP) into the forelimb musculature. After checking for cessation of reflex actions in 10-15 min, the turtles were quickly decapitated via a guillotine. The decapitated head was then skinned on the dorsal side to expose the supraoccipital, parietal, frontal, and the prefrontal bones of the skull. The supraoccipital and parietal bones were fractured. Brain, muscle, and fat tissues were trimmed to expose as much of the bony otic capsule as possible. The entire process of dissection and exposure of the otic capsule was completed in less than 5 min. The otic capsule was opened, and the exposed membranous labyrinth and endolymphatic space of the inner ear flushed with fresh fixative (2% paraformaldehyde, 3% glutaraldehyde, and 1% acrolein in a 0.1M sodium cacodylate buffer) (Appendix 2). The head was immersion fixed in cold, fresh fixative and stored at 4°C for 24 h. The membranous labyrinths were dissected from the otic capsule and transferred to fresh fixative for another 24 h at 4°C. The ears were removed from the fixative, and the utricle and anterior and lateral semicircular ducts were separated from the posterior semicircular ducts, saccule, and cochlear duct. The dorsal wall of the utricle was removed to expose

the otoconial mass. The otoconial mass and the gelatinous membrane beneath it were removed with a fine hair. The utricles were bathed in freshly prepared decalcification solution (2% glutaraldehyde in 0.1 M EDTA and 0.1M sodium cacodylate buffer) (Appendix 2). The tissues were agitated gently for 3 days on a rotator and monitored periodically for the progress of decalcification. The solution was replaced each day. After decalcification, the tissues were processed for LM, TEM, or SEM as follows.

Light Microscopy

Five ears were prepared for LM. The tissues were post-fixed in 1% osmium tetroxide in 0.1 M sodium cacodylate buffer, at 4°C until they became dark brown to black (*ca.* 15 min). These were then dehydrated through a graded series of ethanol solutions of 70%, 75%, 80%, 90%, and 95% for 1 min each followed by two changes in 100% for 1 min. The tissues were transferred twice to 100% propylene oxide for 1 min. They were infiltrated and embedded in Epon (Embed 812, Electron Microscopy Sciences) (Appendix 2). Sections of 1-2.5 μm in thickness were cut with glass knives on a Leica Ultracut UCT ultramicrotome and stained with 1% toluidine blue in sodium tetraborate for 2-5 min. Sections were photographed with a Nikon CoolPix 995 digital camera. Montages of the anterior eighth nerve at different locations along its length provided the nerve fiber counts on 3 specimens. Moreover, a total of 27 nerve fiber diameters were measured in anterior nerve sections at random locations. These sections were from 3 separate specimens. In each of these specimens, 3 large, 3 medium, and 3 small diameter nerve fibers were measured. The measurements were then averaged for each group.

Transmission Electron Microscopy

The blocks prepared for LM were also used for TEM. Ultra thin sections (90-120 nm; silver to gold) were cut with a Diatome diamond knife. The sections were then stained with 2% aqueous uranyl acetate and Reynold's lead citrate. They were viewed and photographed in a Zeiss EM-109 TEM. Approximately 7-10 non-contiguous sections were scanned for the presence of efferent and afferent synapses.

Scanning Electron Microscopy

Attempts were made to clean the surface of the sensory epithelium for SEM viewing. Cleaning involved removal of the otoconial membrane with a fine hair. The tissues were dehydrated in a graded series of ethanol (same as the dehydration protocol above) and critical point dried in a Polaron E 3000 Series critical point dryer (VG Microtech, UK). An approximate 20% tissue shrinkage resulted from the fixation, dehydration, and critical point drying (Bozzolla and Russell, 1999). In the present study, tissue dimensions were not corrected for shrinkage.

The tissues were mounted on metal stubs using colloidal silver paste (Ted Pella, Inc.) so that the macula faced upward. Some of the utricles were flattened to produce fractures in the epithelium. In this way, the basolateral borders of hair cells and nerve fiber profiles might be easily observed. A jet of compressed air was used to remove remaining otoconia and other debris.

Mounted utricles were gold coated in a Hummer II Sputter coater (Technics, Inc.). They were viewed and photographed on a Philips XL40 SEM at the Microscope And Graphic Imaging Center ("MAGIC") at California State University, East Bay. Images were also acquired on a FEI Quanta 200 SEM at San José State University. In some instances, the surface of the macula was scanned for the presence of hair cells from which the hair bundles had been removed. In such cases, a count of stereocilia was obtained.

RESULTS

Gross Morphology of the Inner Ear

The turtle inner ear consists of a pars inferior and superior (Severinsen et al., 2003). The pars inferior contains three sensory epithelia: the basilar papilla, lagenar macula, and saccular macula. The pars superior includes the cristae of the three semicircular ducts and the utricular macula (Figure 4). The utricle is located just ventral to the lateral and anterior cristae (Figure 5).

The Macular Surface of the Utricle (Scanning Electron Microscopy)

The macula of the utricle (neuroepithelium) is concave and covered by a gelatinous or otoconial membrane on which rests the otoconial mass (Figures 6, 7). In the turtle utricle, these otoconia are fusiform-shaped. After removal of most of the otoconial mass and the underlying gelatinous membrane, three regions of the macular surface can be distinguished: a medial cotillus, a striola, and a lateral rampa (Figures 8a, 8b). On the apical surface, these regions are distinguished by the different appearance of hair bundles. These are attached to the overlying gelatinous membrane by their long kinocilia and sometimes by some of the longer stereocilia (Figure 9). Supporting cells with short microvilli on their apical (free) surfaces surround each hair cell.

Striolar Bundles

Bundles in the striolar regions have greater numbers of stereocilia. They are tightly organized in a staggered arrangement. In some cases, the stereocilia in a bundle are organized into a broad oval pattern. In others, the pattern is much narrower. Table 1 presents a count of stereocilia in ten hair bundles. Each bundle has an average of 65 stereocilia. The kinocilium is much shorter than that found in the extrastriolar regions (Figures 10a, 10b). An average of 58 (Table 1) stereocilia per hair bundle was calculated in the region adjacent to the striola (juxtastriola) ($n = 3$). The kinocilia in the juxtastriolar region extend beyond the tallest members of the bundle but are not as long as kinocilia found in the extrastriolar regions (Figure 10b).

In turtle striolar bundles the kinocilial bulb contacts the tallest row of stereocilia. The kinocilium is taller than the bundle, and its curved portion is easily observed (Figure 10a). In the same micrograph, the tapered ends of the stereocilia are evident as they enter the apical surface of the hair cell.

Extrastriolar Bundles

The overall shape of the hair bundles in the rampa and cotillus is in a narrow oval, unlike those in the striolar region. Bundles in the lateral extrastriolar region (rampa) generally have fewer stereocilia than those in the striola. Kinocilial height is greater, with some bundles having kinocilia 3-5 times as long as the tallest stereocilia in the bundle (Figures 11a, 11b). An average of 45 stereocilia per bundle was observed in five

hair bundles in the rampa (Table 1). In some micrographs, the filamentous network of the otoconial membrane is visible.

Bundles in the medial extrastriolar region (cotillus) have fewer stereocilia than in striolar bundles. The hair bundles are long, slim, and cigar-shaped. The kinocilium is much longer (*ca.* three times) than the tallest stereocilium in the bundle (Figure 12). An average of 66 stereocilia per bundle was observed in five hair bundles in the cotillus. As elsewhere, the surface of supporting cells is characterized by the presence of a single ciliary rod in its center (Figure 12).

Light Microscopy and Transmission Electron Microscopy of the Macula

The sensory organ is organized into three layers from top to bottom: otoconia, a gelatinous membrane, and the sensory epithelium (Figure 13). The epithelium consists of supporting cells, hair cells, and branches of the anterior portion of the eighth cranial nerve.

Supporting Cells

Supporting cells surround the hair cells and, in most cases, span the height of the macula. On the apical surface are numerous microvilli (Figure 14) and sometimes a single, central ciliary rod. The basal side of the supporting cell sits on a basement membrane separating the epithelium from the underlying connective tissue and nerve. A prominent ultrastructural feature of supporting cells is the presence of electron-dense granules (Figure 14). These, often irregularly shaped, granules are bounded by an

electron-dense membrane. Mitochondria and Golgi bodies are found in the cytoplasm. Another prominent feature is the extensive infolding of the cell membrane. Junctional complexes (Figures 14, 16) are composed of tight junctions, intermediate junctions, and desmosomes and are present between supporting cells and between supporting cells and hair cells.

Hair Cells

Stereociliary bundles, as described earlier, occur on the apical surfaces of these cells. The stereocilia are not true cilia, lacking the typical 9+2 arrangement of microtubules. Their cytoplasm is packed with thin filaments. Filamentous connections can be observed between stereocilia in some preparations (Figure 15). The kinocilium is a true cilium and is characterized by the typical 9+2 arrangement of microtubules. The entire hair bundle is attached to the hair cell in a region known as the cuticular plate (Figure 16). Each stereocilium tapers where it connects to the plate.

Also present on the hair cell are afferent synapses. The afferent synaptic body, located within the hair cell cytoplasm, consists of a dense spherical body surrounded by a halo of vesicles (Figure 17). The synaptic body and surrounding vesicles are closely associated with a section of the pre-synaptic membrane that is thickened and stains more densely than the adjacent membrane (Figure 17). The postsynaptic membrane of the afferent terminal is also thickened.

A cellular process containing numerous membrane-bound vesicles and mitochondria was observed to be in contact with an adjacent hair cell and the thin cellular processes of

nearby supporting cells (Figure 18). No membrane thickenings or membrane-associated structures were observed in this plane of section. No other vesicle filled processes were observed in approximately 7-10 sections.

Vestibular Nerve

The anterior branch of the vestibular nerve innervates hair cells in the utricular epithelium (Figure 19a). The tracing (Figure 19b) shows the relative positions of the anterior crista and utricular macula. The ampullary division of the anterior eighth nerve is composed of branches of nerve fibers arising from the lateral and anterior cristae ampullares. Three branches usually arise from the anterior and two from the lateral cristae. They combine ventral to the two ampullae, and the nerve fibers from the utricular macula join the anterior nerve at this location. The anterior ganglion is present ventral to the utricle.

Terminal branches of afferent and efferent nerve fibers within the epithelium are usually unmyelinated (Figure 20). Rarely, thinly myelinated, large diameter nerve fibers occur within the neuroepithelium (Figure 21). Most myelinated afferent axons gain their myelin sheaths when they exit the epithelium (Figure 22). Associated with myelinated axons are cells with a denser cytoplasm, most likely Schwann cells (Figures 22, 23). The endoneurium of the nerve (connective tissue enveloping each nerve fiber) contains many collagen fibrils (Figure 23). In one profile, the myelin sheath was thick and contained *ca.* 73 layers of myelin (Figure 24).

Also present in the anterior branch of the eighth cranial nerve are cell bodies that form the anterior ganglion (Figures 25, 26, 27). The nerve also contains blood vessels, including various capillary profiles (Figures 26, 28). Mast cells (Figure 29) are also found in the connective tissue surrounding the nerve fibers.

Light micrographs of the anterior nerve and the ampullary division (from the anterior and lateral cristae) were obtained at locations shown in Figure 19b (Figures 30a, 30b). Counts of nerve fibers were made from montages of light micrographs at higher magnifications (*ca.* 800x). The number of nerve fibers innervating the utricular epithelium was then estimated using the following equation:

$$\text{no. of fibers innervating utricle} = \text{anterior nerve} - (\text{lateral ampullary nerve} + \text{horizontal ampullary nerve})$$

The counts obtained from three specimens are compiled in Table 3. The nerves from the lateral and anterior cristae had an average of 744 and 808 nerve fibers, respectively. The anterior branch of the eighth nerve contained an average of 2,814 fibers. By means of the above formula, the average number of nerve fibers arising from the utricle was calculated to be 1,263.

The diameter of 27 nerve fibers in the anterior eighth nerve was measured in three specimens and ranged from 2.8 to 7.4 μm (Table 4). On visual inspection of large, medium, and small diameter fibers, no pattern of distribution was evident. The three groups of nerve fibers were also present in the branches from the anterior and lateral cristae.

DISCUSSION

Utricular Macula

Surface and Hair Bundle Morphology

The present study adds to the information concerning the structure of the turtle utricle. The gross anatomy and ultrastructure of the utricular macula are similar to those of other vertebrates (Severinsen et al, 2003; Fontilla and Peterson, 2000). The present study adds to the few SEM images of the utricular otoconia (Ross and Pote, 1984; Lychakov, 2004) and includes the first SEM images of the underlying otoconial membrane in reptiles. The surface of the utricular macula can be segregated into three regions on the basis of hair bundle morphology: striola, rampa, and cotillus. A prominent bulb at the tips of kinocilia of striolar as well as juxtastriolar hair bundles suggests a strong attachment to the overlying otoconial membrane. Often the kinocilium in each striolar hair bundle is bent so that the bulb rests on rows of taller stereocilia. The function of this particular organization has not been discussed in the literature. It may provide stronger interaction between the rows of longer stereocilia and kinocilium and the overlying otoconial membrane. In the bullfrog, hair cells in the striolar region are more sensitive to stimulation than extrastriolar hair cells (Baird, 1994). Furthermore, hair cells in the medial striolar rows (type E) have vibratory sensitivity. These hair cells are characterized by a prominent kinocilial bulb and a kinocilium not much longer than the stereocilia (Baird and Lewis, 1986). Hair cells with numerous short stereocilia are most sensitive because a greater number of stereocilia implies more transducer channels (Baird, 1994). A similar line of reasoning can be applied to striolar (and juxtastriolar) hair bundles in the

turtle. In addition, as suggested in the bullfrog utricle, the sensitivity of the hair cell and afferent nerve fiber is determined by the nature of the mechanical coupling between the stereociliary bundle and the overlying otoconial membrane. Hair cells that are rigidly coupled to the otoconial membrane are responsive to its displacement (Baird and Lewis, 1986). Similarly, a stronger region of attachment to the overlying membrane would increase displacement of the bundle, hence increasing sensitivity to stimulation.

The number of stereocilia and lengths of the kinocilia in representative hair bundles from different regions of the macula was obtained. In the rampa, the number of stereocilia (average of 45 per bundle) was similar to that obtained by Severinsen et al. (2003) and Moravec and Peterson (2004) (average of 38 and 42 per bundle, respectively) (Table 2). Striolar hair bundles in the turtle have more (average of 65 per bundle) stereocilia. Severinsen et al. (2003) reported similar numbers. Furthermore, Moravec and Peterson (2004) have reported that the number of stereocilia in hair bundles in the striolar region depends on whether a type I hair cell or a type II hair cell bundle is counted. Striolar type I hair bundles have more stereocilia (average of 96 per bundle) than striolar type II hair cell bundles (average of 60 per bundle) (Moravec and Peterson, 2004). Hence, the bundles counted in the present study may belong to type II hair cells. However, there were two hair bundles containing 84 and 89 stereocilia. These could be type I hair cell bundles according to the data of Moravec and Peterson (2004). Stereociliary numbers in cotillary hair bundles in the present study were greater (average of 67 per bundle) than the numbers reported by Severinsen et al. (average of 44 per bundle) (2003) and Moravec and Peterson (average of 54 per bundle) (2004) (Table 2).

The discrepancy between the counts may be due to the extremely high value of 106 stereocilia counted in one of the cotillary bundles, skewing the results. The stereociliary count for this hair cell may also have included nearby microvilli on the hair cell surface.

A complete count of hair cell numbers could not be obtained because the otoconial membrane obstructed the surface of the macula. In addition, many hair bundles were lost during the sample preparation process.

Epithelial Ultrastructure

Some ultrastructural features of the utricular macula in turtles have been described (Jorgensen, 1974). Jorgensen (1974) described the two types of hair cells (type I and type II) in the utricular epithelium in two turtle species (*Testudo graeca* and *Pseudemys scripta*) based on light and electron microscopic observations. In addition, he described the morphological polarization of hair bundles on the macular surface. The present study provides more detail and reveals structures and specializations present in the utricular epithelium similar to those reported in mammals (Kirkegaard and Jorgensen, 2001). The hair cell cytoplasm is filled with mitochondria and vesicles. Each hair cell has a bundle of stereocilia and a single kinocilium on its apical surface. Supporting cell membranes are thrown into folds that interdigitate with adjacent hair cells and supporting cells. The reticular membrane described in mammals (Kirkegaard and Jorgensen, 2001; Oesterle et al., 2003) was not observed in the present study and is not known to be present in reptilian utricular macula. In mammals, this membrane is visualized as a dark band below the apical surface of supporting cells and consists of densely packed actin

filaments (Oesterle et al., 2003). Furthermore, the electron-dense, membrane-bound granules ringed by ribosomes, described in the cytoplasm of mammalian supporting cells, are also present in the turtle. There are several hypotheses for the formation of otoconia (Tateda et al., 1998). One of them suggests that the globular substance found in the otoconial membrane of invertebrates, birds, and mammals is a precursor of otoconia and is secreted by the supporting cells of the macula. This globular substance then crystallizes to mature otoconia in the meshwork of the otoconial membrane (Suzuki et al., 1995). The membrane-bound granules described above and in the turtle supporting cells may be the source of this globular substance.

Efferent nerve fiber synapses in the utricle of the turtle have not been described. However, the efferent synapse in mammals has been well described (Oesterle et al., 2003; Lysakowski and Goldberg, 1997; Kirkegaard and Jorgensen, 2001). In the rat utricle, a bouton nerve ending filled with numerous vesicles characterizes the efferent synapse. A cistern of the smooth endoplasmic reticulum is often located in the post-synaptic hair cell. The cellular process in contact with an adjacent hair cell that was observed in the present study was filled with numerous vesicles and mitochondria. However, it did not show any pre- or post-synaptic thickenings or a sub-synaptic cistern in the post-synaptic hair cell. This may be because these membrane specializations were located above or below the plane of the ultra-thin section. Hence, this process may have been an efferent nerve bouton or a portion of a dimorphic bouton contacting the hair cell. Further TEM analysis of ultra-thin sections needs to be carried out to confirm the presence and morphology of efferent synapses in the turtle utricular macula.

Efferent synaptic elements have been described in the crista ampullares of the chinchilla (Lysakowski and Goldberg, 1997). The efferent synaptic contacts on type II hair cells are characterized by the presence of a post-synaptic cistern of the endoplasmic reticulum, whereas efferent synapses with calyces and other afferent processes are characterized by the presence of slight presynaptic and postsynaptic thickenings.

Vestibular Nerve

Gross Anatomy

The anatomy of the anterior branch of the eighth nerve observed in the turtle is similar to that observed in another reptile, *Caiman crocodilus* (Leake, 1974). However, an observation made in this study that has not been discussed previously is the presence of more than one ampullary branch arising from the lateral and anterior semicircular cristae.

Light Microscopy and Transmission Electron Microscopy

Large, medium, and small populations of myelinated nerve fibers were visualized in the anterior branch of the eighth nerve. These fibers were distributed randomly in the nerve and ranged from 2.8 to 7.4 μm in diameter (including the myelin sheath). A random distribution of similar fibers was also observed in the branches from the anterior and lateral cristae. Therefore, the measured nerve fibers could have come from any of the three regions (anterior or lateral cristae or the utricular macula). These values were similar to values obtained in the pigeon and human anterior nerves. In pigeons, vestibular afferents range from 0.54 to 8.2 μm in diameter (Si et al., 2003). Lopez et al.

(2005) investigated the anterior division of the eighth nerve in humans and reported a similar range of diameters.

In the present study, the total number of nerve fibers (afferent + efferent) in the ampullary, utricular, and anterior branches of the eighth nerve has been reported for the first time in reptiles. The total number of nerve fibers (afferents and efferents) in the utricle was 1,263. Observations were conducted at the LM level, and so the presence or absence of unmyelinated fibers could not be confirmed. Still, no unmyelinated profiles were observed in LM montages of the entire nerve or TEM images of the nerve. This suggests that both afferent and efferent fibers are myelinated in the turtle. An error in the total number of nerve fibers could arise because of the plane of section. In some cases, a single fiber could be counted multiple times if it coursed back and forth through the same plane of section. This probably did not occur often, but a few profiles indicated that it might have. If the total number of hair cells in the mature turtle utricular macula is estimated to be *ca.* 10,000 (Severinsen et al., 2003), then the nerve fiber to hair cell ratio is 1:8, that is, one nerve fiber innervating approximately eight hair cells in the macula.

The number of nerve fibers innervating the utricle in turtles was less than that innervating the bullfrog (2,315) (Baird and Schuff, 1994), or human (3,023) (Lopez et al., 2005). A comparison of the number of nerve fibers innervating the utricle in different species is presented in Table 3.

Another study conducted by Gopen et al. (2003) reported 27,508 hair cells in human utricular maculae of which 17,326 were type I hair cells and 10,182 were type II hair

cells. Therefore, the ratio of nerve fibers to hair cells in the human utricular macula is approximately 1:10.

In their study of the bullfrog utricle, Baird and Schuff (1994) observed that, in the extrastriolar and juxtastricular afferents, each hair cell could be contacted by as many as four synaptic endings from a given afferent. This gives a ratio of 2 synaptic endings per hair cell. On the other hand, in the striolar region, each hair cell could be contacted by as many as 15 synaptic endings from a given afferent, for a ratio of 5 synaptic endings per hair cell. In the pigeon utricle, 6 type I hair cells were observed per calyx and an average of 7 type I hair cells per afferent nerve fiber. In the dimorphic afferents, averages of 4 type I hair cells per calyx, 5 type I hair cells per fiber, and 17 boutons were observed per afferent nerve fiber. In the same study, an average of 60 bouton terminals per afferent nerve fiber was observed (Si et al., 2003).

The average number of nerve fibers and hair cells in the utricular maculae of *Trachemys scripta elegans* is less than that in humans (Gopen et al., 2003). A trend of increasing number of nerve fibers innervating the utricular macula is seen from reptiles (turtle) to amphibians (bullfrog) to mammals (human). However, the ratio of nerve fibers to hair cells is similar, suggesting that, although the number of hair cells increased from reptiles to humans, the level of complexity of innervation was conserved evolutionarily. Hence, this species of reptiles can be used to study structure/function relationships in general.

Future Directions

The morphology of the reptile utricle has been ignored. For instance, a more thorough investigation of the formation of the gelatinous membrane and otoconia is needed. A more accurate estimate of the number of afferent nerve fibers could be obtained by counting the number of anterior ganglion cells. This number can be subtracted from the count of total nerve fibers to give the number of efferent fibers present. Furthermore, serial section analysis may be used to determine the number and pattern of innervation of afferent and efferent nerve fibers. The ratio of number of hair cells to afferent nerve fibers needs to be determined across the various regions of the macula as well as across age groups to determine whether it changes with region and age. Nerve innervation patterns for the reptilian utricular macula have not been studied so far. Unbiased stereology, immunocytochemistry, tracer dye injections as well as serial section analysis can be conducted to analyze the innervation patterns (Lopez et al., 2005; Si et al., 2003; Baird and Schuff, 1994).

BIBLIOGRAPHY

Baird RA, Lewis ER. Correspondences between afferent innervation patterns and response dynamics in the bullfrog utricle and lagena. *Brain Res* 1986; 369:48-64.

Baird RA, Schuff NR. Peripheral innervation patterns of vestibular nerve afferents in the bullfrog utricle. *J Comp Neurol* 1994; 342:279-298.

Baird RA. Comparative transduction mechanisms of hair cells in the bullfrog utricle. I. Responses to intracellular current. *J Neurophysiol* 1994; 71(2):666-684.

Barbas-Henry HA, Lohman AHM. Primary projections and efferent cells of the VIIIth cranial nerve in the monitor lizard, *Varanus exanthematicus*. *J Comp Neurol* 1988; 277:234-249.

Bozzolla JJ, Russell LD. *Electron microscopy: principles and techniques for biologists*. 2nd ed. Sudbury, MA. Jones and Bartlett. 1999.

Colclasure JC, Holt JR. Transduction and adaptation in sensory hair cells of the mammalian vestibular system. *Gravitation Space Biol Bull* 2003; 16(2):61-70.

Desai SS, Zeh C, Lysakowski A. Comparative morphology of rodent vestibular periphery: I. Saccular and utricular maculae. *J Neurophysiol* 2005; 93(1):267-280.

Fontilla MF, Peterson EH. Kinocilia heights on utricular hair cells. *Hearing Res* 2000; 145:8-16.

Frolenkov GL, Belyantseva IA, Friedman TB, Griffith AJ. Genetic insights into the morphogenesis of inner ear hair cells. *Nature Reviews* 2004; 5:489-498.

Gopen Q, Lopez I, Ishiyama G, Baloh RW, Ishiyama A. Unbiased stereologic type I and type II hair cell counts in human utricular macula. *Laryngoscope* 2003; (Abstract)

Harada Y, Kasuga S, Tamura S. Comparison and evolution of the lagena in various animal species. *Acta Otolaryngol* 2001; 121:355-363.

Jorgensen JM. The sensory epithelia of the inner ear of two turtles, *Testudo graeca* L and *Pseudemys scripta* (Schoepff). *Acta Zoologica* 1974; 55:289-298.

Kirkegaard M, Jorgensen JM. The inner ear macular sensory epithelia of the Daubenton's bat. *J Comp Neurol* 2001; 438:433-444.

Ladich F, Popper AN. Comparison of the inner ear ultrastructure between teleost fishes using different channels for communication. *Hearing Res* 2001; 154(1-2):62-72.

Leake PA. Central projections of the statoacoustic nerve in Caiman crocodiles. *Brain Behav Evol* 1974; 10:170-196.

Lins U, Farina M, Kurc M, Riordan G, Thalmann R, Thalmann I, Kachar B. The otoconia of the guinea pig utricle: internal structure, surface exposure, and interactions with the filament matrix. *J Struct Biol* 2000; 131:67-78.

Lopez I, Ishiyama G, Tang Y, Frank M, Baloh RW, Ishiyama A. Estimation of the number of nerve fibers in the human vestibular endorgans using unbiased stereology and immunohistochemistry. *J Neurosci Meth* 2005; 145:37-46

Lu Z, Xu Z, Buchser WJ. Coding of acoustic particle motion by utricular fibers in the sleeper goby, *Dormitator latifrons*. *J Comp Physiol* 2004; 190:923-938.

Lychakov DV. Evolution of otolithic membrane. Structure of otolithic membrane in amphibians and reptilians. *J Evol Biochem Phys* 2004; 40(3):331-342.

Lysakowski A, Goldberg JM. A regional ultrastructural analysis of the cellular and synaptic architecture in the Chinchilla cristae ampullares. *J Comp Neurol* 1997; 389:419-443.

Moravec WJ, Peterson EH. Differences between stereocilia numbers on type I and type II vestibular hair cells. *J Neurophysiol* 2004; 92:3153-3160.

Oesterle EC, Cunningham DE, Westrum LE, Rubel EW. Ultrastructural analysis of [³H] thymidine-labeled cells in the rat utricular macula. *J Comp Neurol* 2003; 463:177-195.

Platt C, Jorgensen JM, Popper AN. The inner ear of the lungfish *Protopterus*. *J Comp Neurol* 2004; 471:277-288.

Severinsen SA, Jorgensen JM, Nyengaard JR. Structure and growth of the utricular macula in the inner ear of the slider turtle *Trachemys scripta*. *J Assoc Res Otolaryngol* 2003; 4:505-520.

Si X, Mridha MD, Zakir, Dickman JD. Afferent innervation of the utricular macula in pigeons. *J Neurophysiol* 2003; 89:1661-1677.

Sneary MG. Auditory receptor of the red-eared turtle: II. Afferent and efferent synapses and innervation patterns. *J Comp Neurol* 1988; 276:588-606.

Sondag E. The effects of hypergravity on function and structure of the peripheral vestibular system. University of Amsterdam, Ph.D. Thesis 1996.

Styeger PS, Wiederhold ML. Visualization of newt aragonitic otoconial matrices using transmission electron microscopy. *Hearing Res* 1995; 92:184-191.

Tateda M, Suzuki H, Ikeda K, Takasaka T. pH regulation of the globular substance in the otoconial membrane of the guinea-pig inner ear. *Hearing Res* 1998; 124:91-98.

Xue J, Peterson EH. Hair bundle heights in the utricle: differences between macular locations and hair cell types. *J Neurophysiol* 2006; 95:171-186.

APPENDIX 1: FIGURES AND TABLES

LIST OF FIGURES

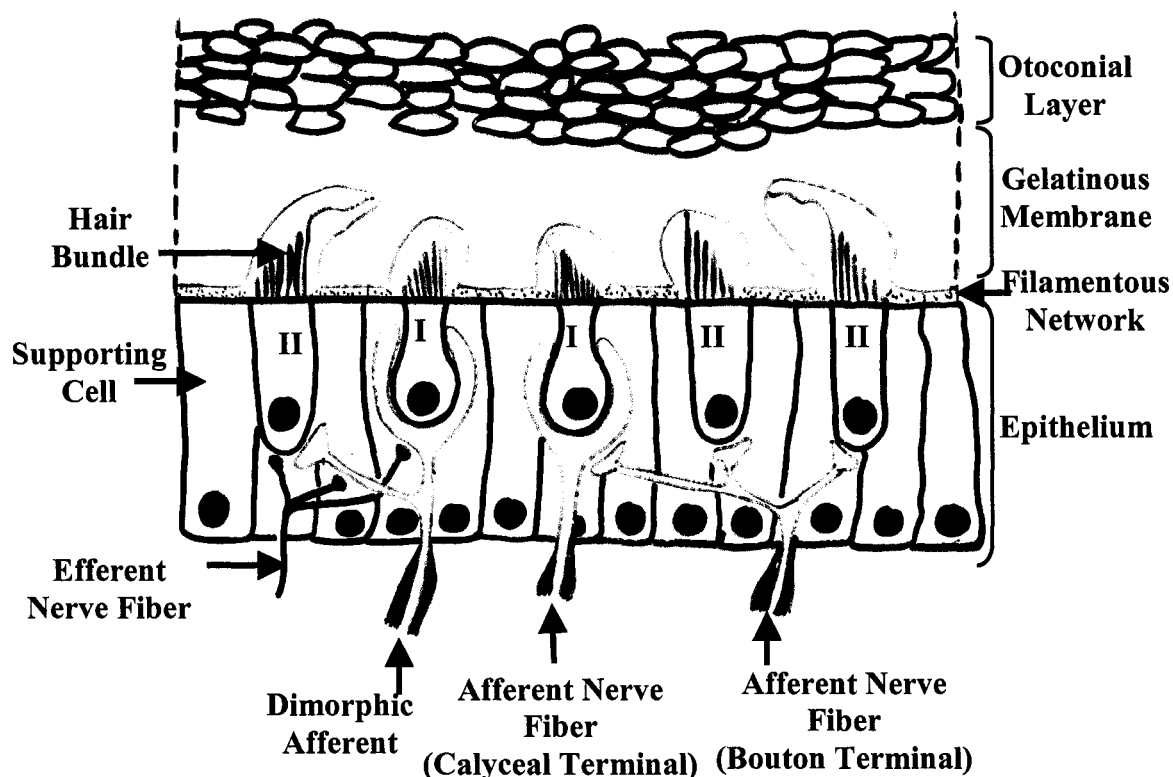


FIGURE 1. Schematic cross-sectional diagram of the utricle. The sequential layers of the otoconial (inertial) mass, gelatinous membrane, and the epithelium can be seen. There is a filamentous network between the gelatinous membrane and the apical surface of the epithelium in areas where the hair bundles are absent. The hair bundles are attached to the overlying gelatinous membrane. The epithelial layer consists of two types of cells: supporting cells and hair cells. Two types of hair cells are present: Type I (I) and type II (II). Both types have characteristic shapes, hair bundle morphologies and nerve fiber contacts. Type I hair cells are contacted by calyceal afferent terminals. These engulf the basolateral surface of the target hair cell. Type II hair cells are contacted by bouton terminals. Some afferent endings are dimorphic having both calyceal and bouton endings. Afferent nerve fibers have greater diameters than efferent fibers. Both gain their myelin sheaths after they exit the epithelium.

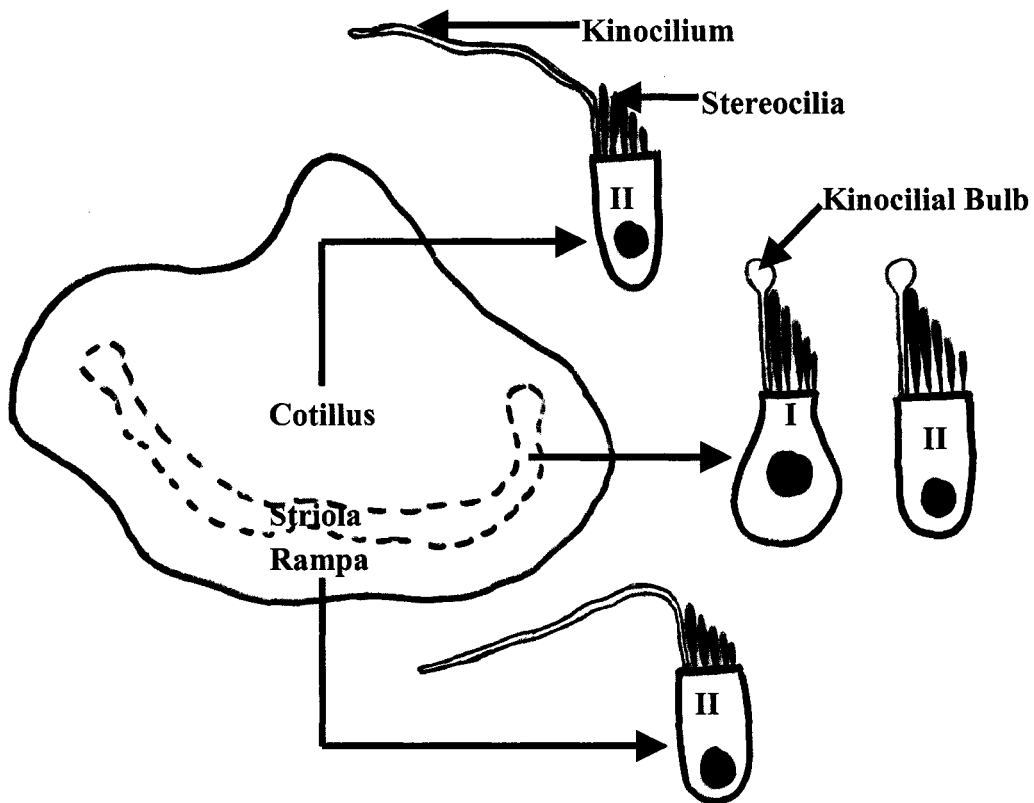


FIGURE 2. Diagram of the utricular macular hair cell populations. Different regions of the macula have different hair cell morphologies. The rampa and the cotillus have hair cells each with a long kinocilium and numerous short stereocilia. In this region only type II hair cells are found. The striola has hair cells each with a short kinocilium and many more stereocilia than in either the rampa or cotillus. The striola has both type I and type II cells.

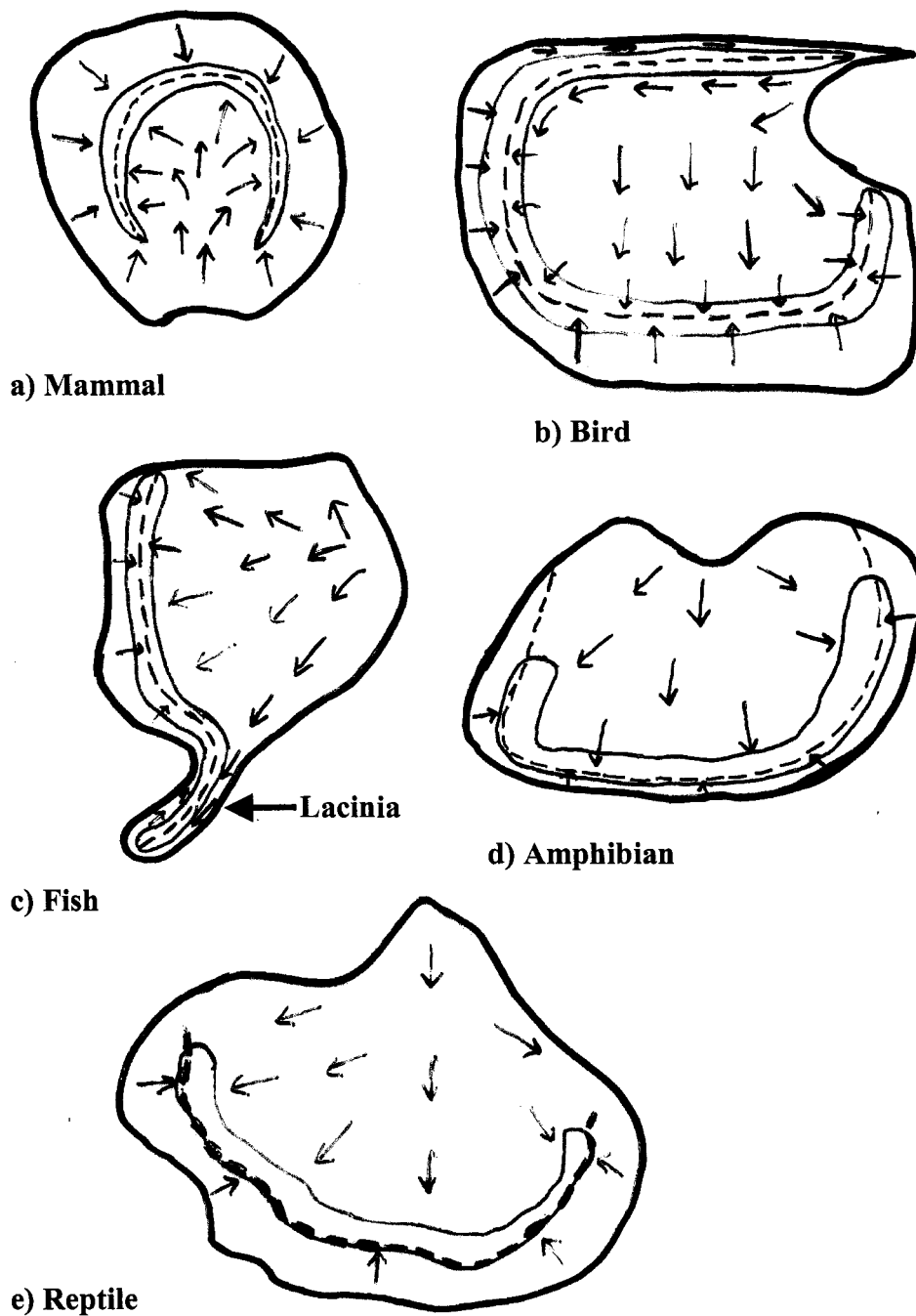


FIGURE 3. Macular shape and hair bundle orientation patterns of various species. The arrows show the direction of hair bundle orientation. — : Outline of the striola, -----: line of polarity reversal.

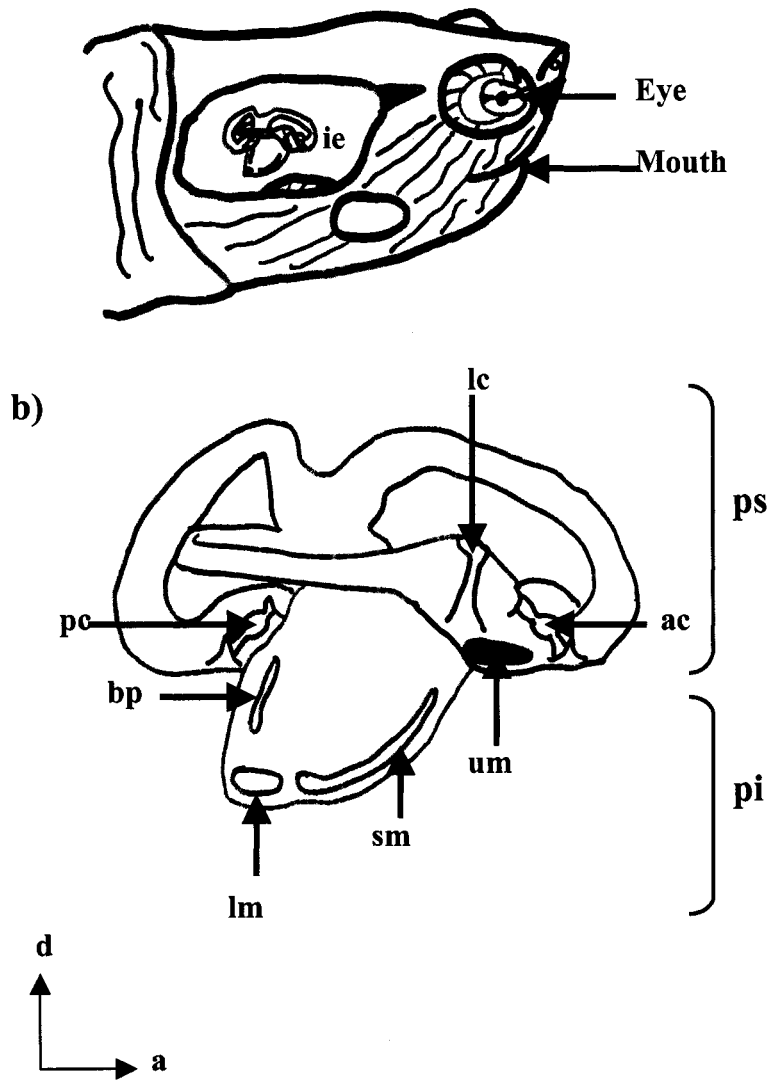


FIGURE 4. (a) Relative position of the inner ear. (b) Lateral view of the inner ear (*ie*) and the relative positions of the sensory end organs are shown. *ac*: anterior crista; *lc*: lateral crista; *pc*: posterior crista; *bp*: basilar papilla; *lm*: lagenar macula; *sm*: saccular macula; *um*: utricular macula; *ps*: *pars superior*; *pi*: *pars inferior*; *d*: dorsal direction; *a*: anterior direction. Adapted from Severinsen et al., 2003.

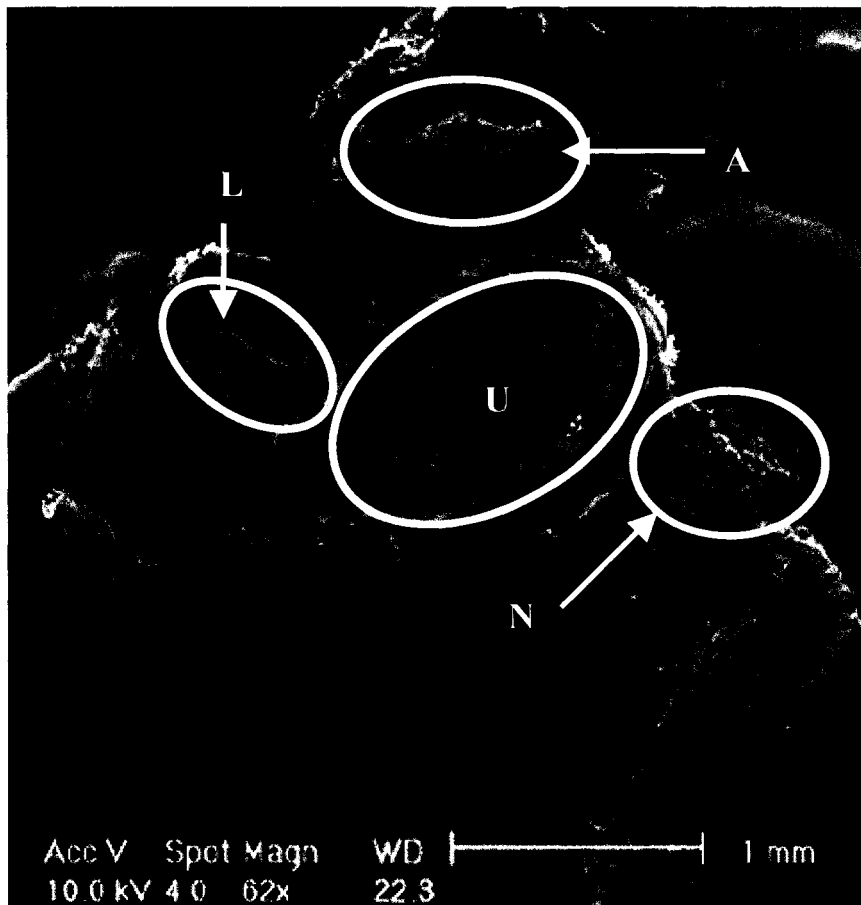


FIGURE 5. SEM of the utricle and semicircular cristae surfaces. The micrograph shows the location of the utricle (U) as ventral to the anterior (A) and lateral (L) semicircular cristae. A portion of the anterior branch of the eighth cranial nerve (N) innervates the utricular macula and the cristae.

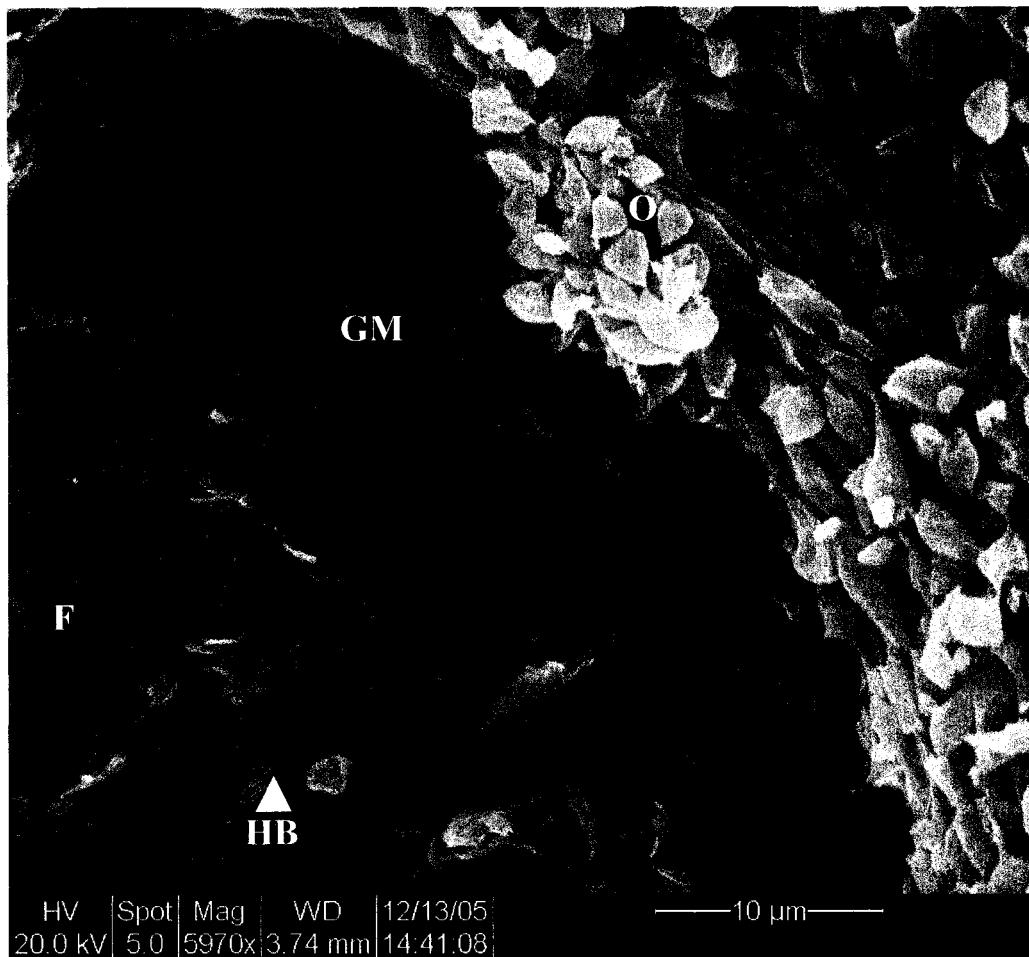


FIGURE 6. SEM of the macula and overlying layers. The otoconial layer (O) is the topmost layer in contact with the endolymph. The underlying layer is the gelatinous membrane (GM), the lower part of which is in contact with hair bundles (HB). F: filamentous network.

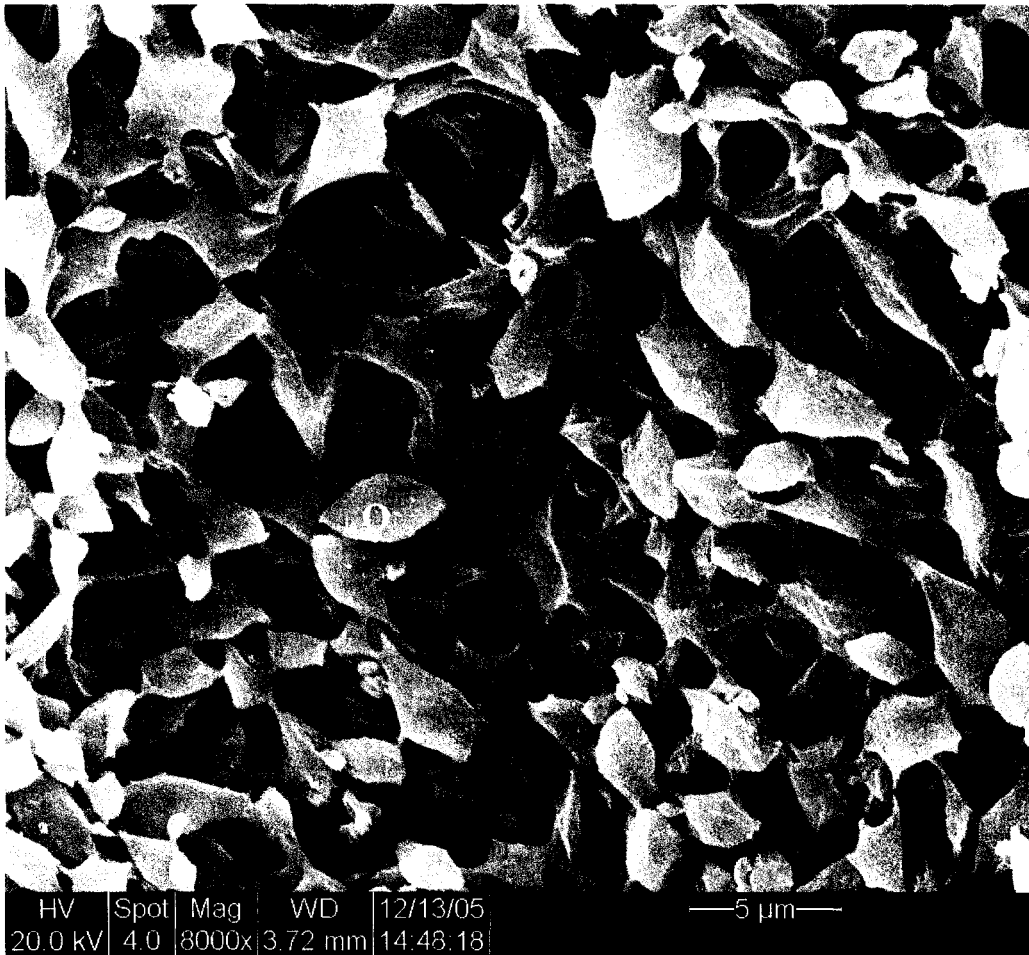


FIGURE 7. SEM of the otoconial layer. The individual otoconia (O) have a distinct fusiform shape.

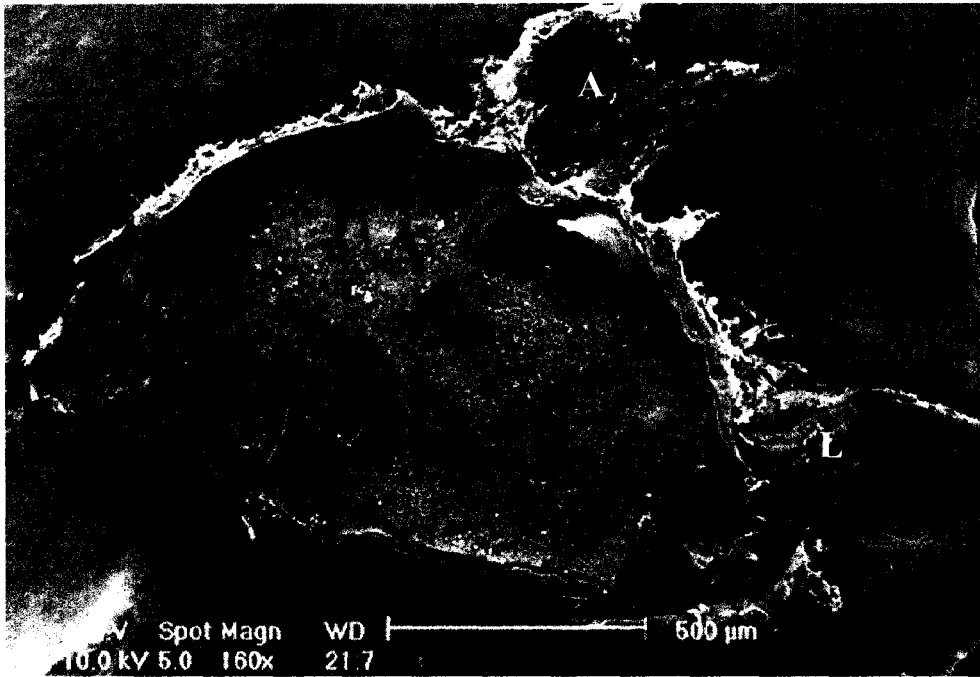


FIGURE 8a. SEM of the surface of the utricle. The otoconial layer and the gelatinous membrane have been removed. Remnants of the branches of the eighth nerve from the lateral (L) and anterior (A) cristae can also be seen.

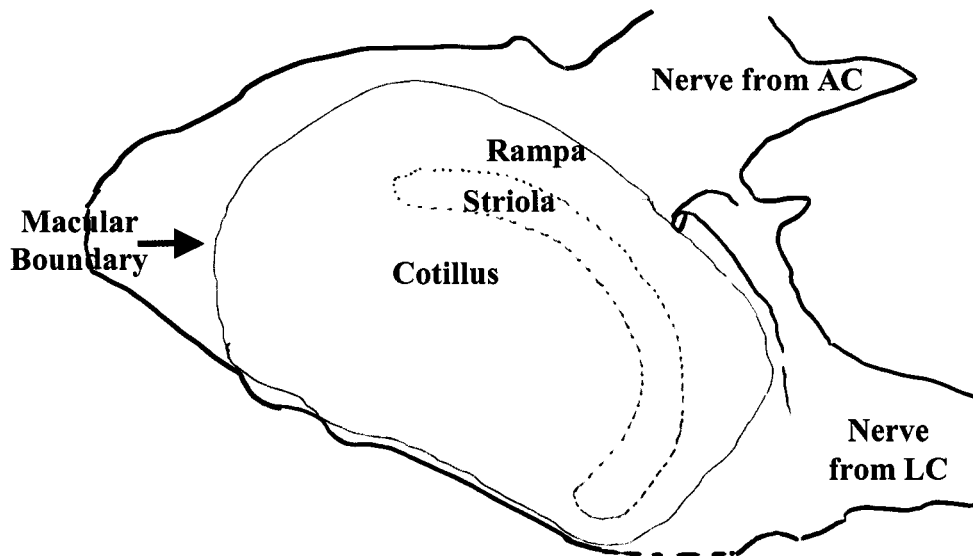


FIGURE 8b. A tracing of the utricular macular surface. It indicates the lateral extrastricular region (rampa), medial extrastricular region (cotillus), and striola. AC: anterior crista, LC: lateral crista.



FIGURE 9. SEM of the attachment of a hair bundle to the overlying membrane (arrow). This cell is in the rampa. In this specimen the apparent tension in this contact is most likely an artifact of critical point drying.

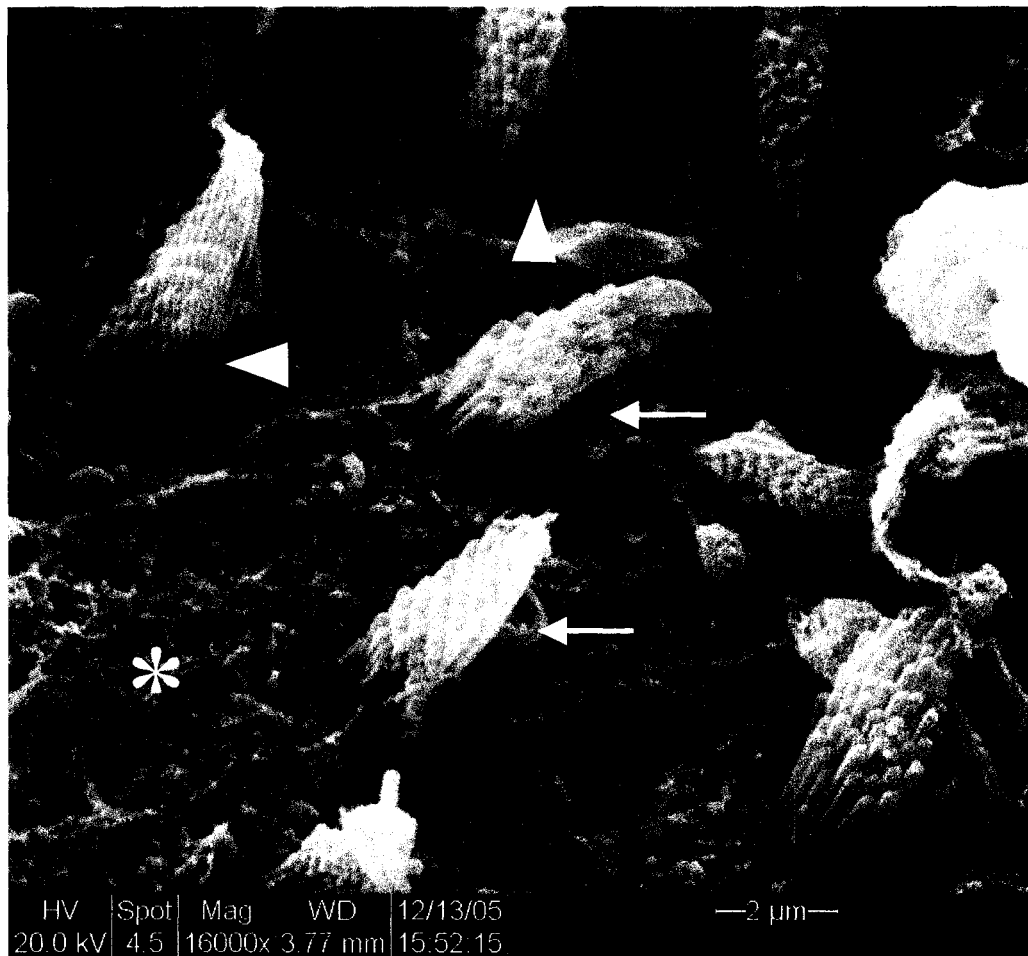


FIGURE 10a. SEM of striolar hair bundles. Notice the numerous stereocilia arranged in staggered rows and the bent kinocilia (arrows). The kinocilia have a bulb that is attached to the rows of the tallest stereocilia in each hair bundle. The filamentous network on the surface of the epithelium can also be seen (asterisk). The arrowheads indicate the region of each stereocilium where they taper.

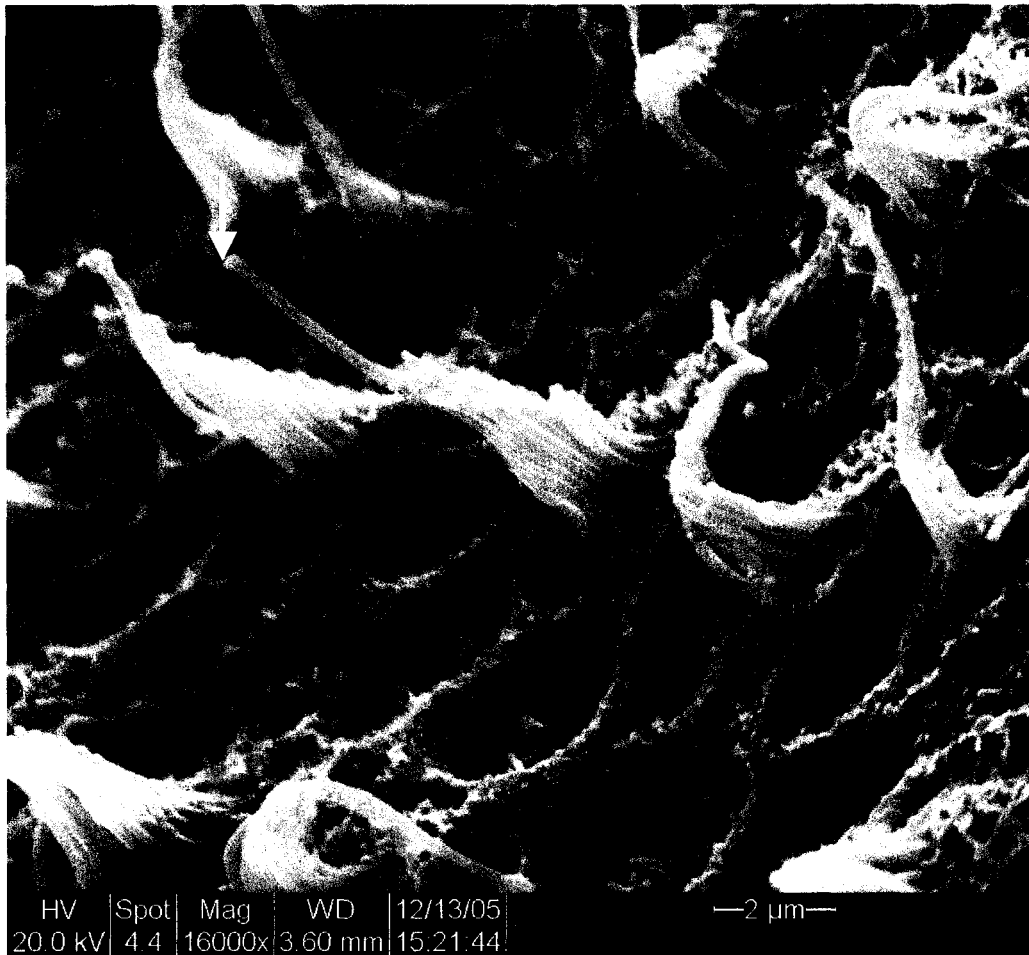


FIGURE 10b. SEM of juxtastricular hair bundles. Notice that the kinocilium is straight and extends beyond the tallest stereocilia in the bundle and that it has a small bulb.

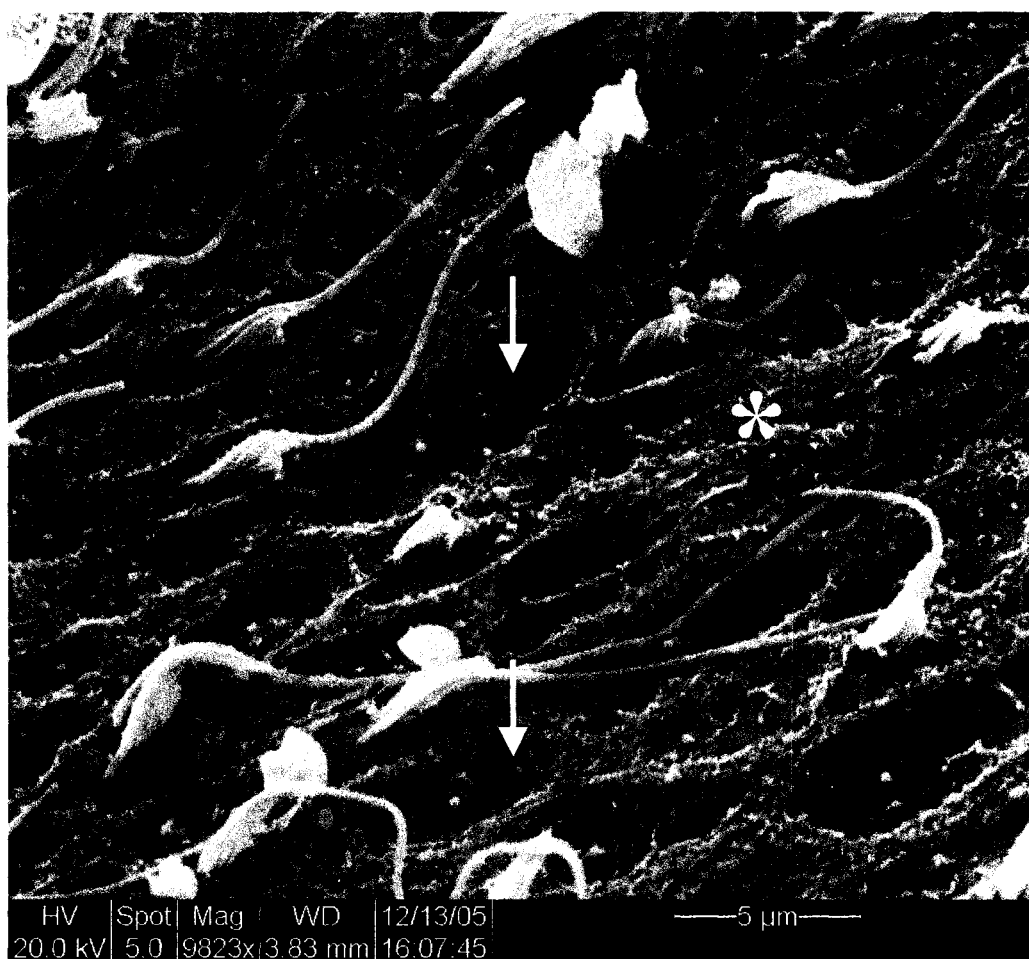


FIGURE 11a. SEM of rampary hair bundles. Also visible are supporting cells (arrows), each with a characteristic central ciliary rod. The asterisk points out the filamentous network.

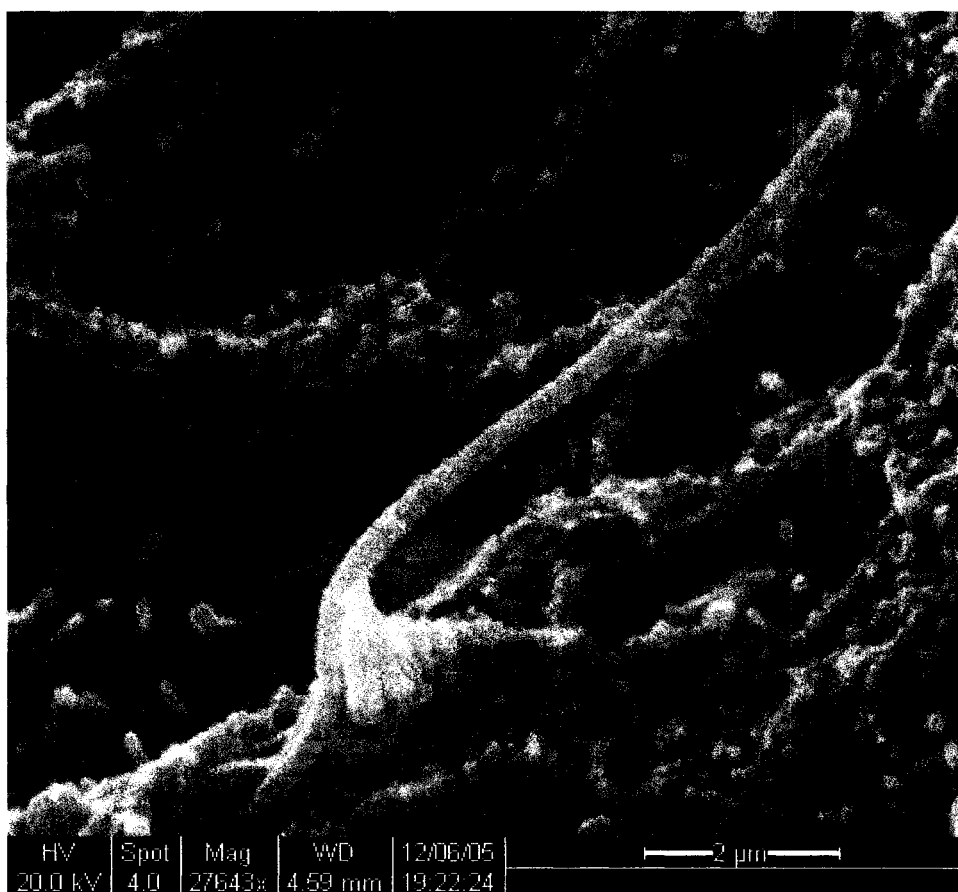


FIGURE 11b. SEM of rampary hair bundle. The hair bundle has few stereocilia and the kinocilium is three-to-five times longer than the tallest stereocilium in each bundle.

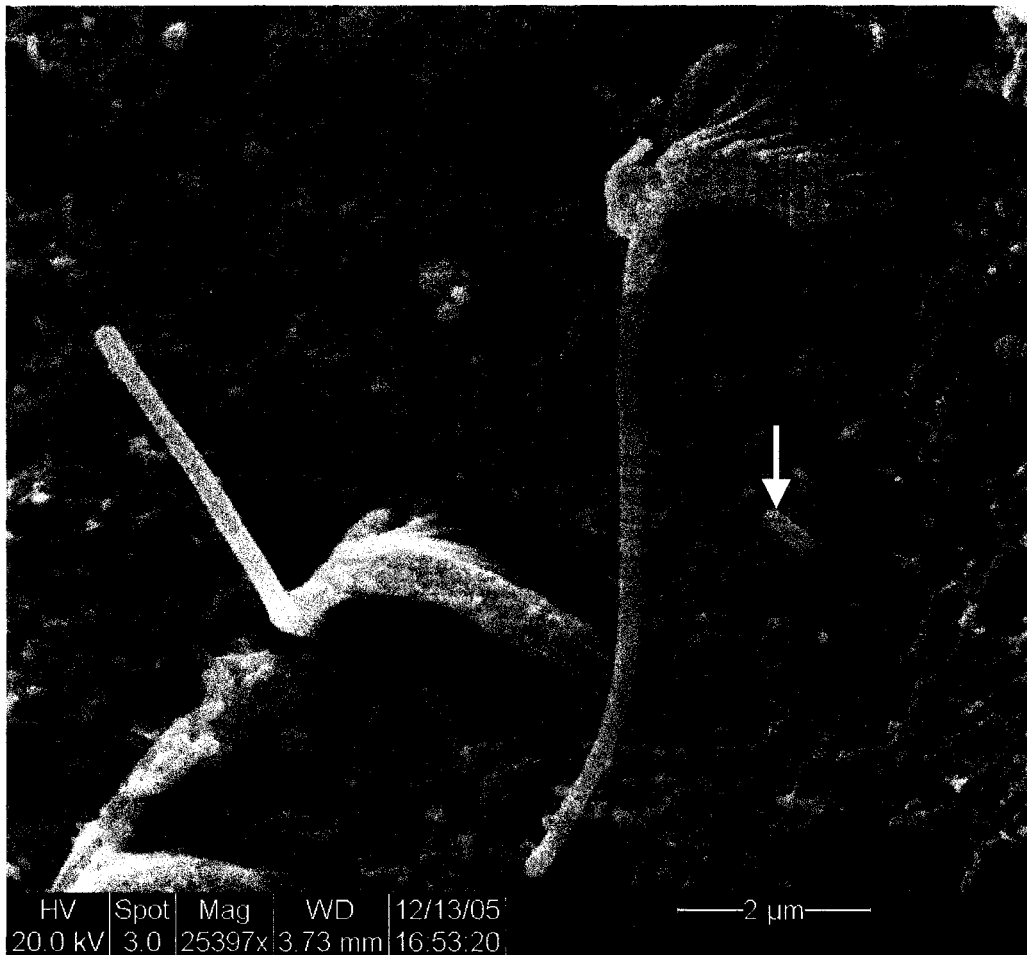


FIGURE 12. SEM of cotillary hair bundles. The hair bundles in this region have few stereocilia and a kinocilium that is much longer than the tallest stereocilia in the bundle. Note the “cigar shape” of the bundles. Arrow: central ciliary rod on the surface of a neighboring supporting cell.

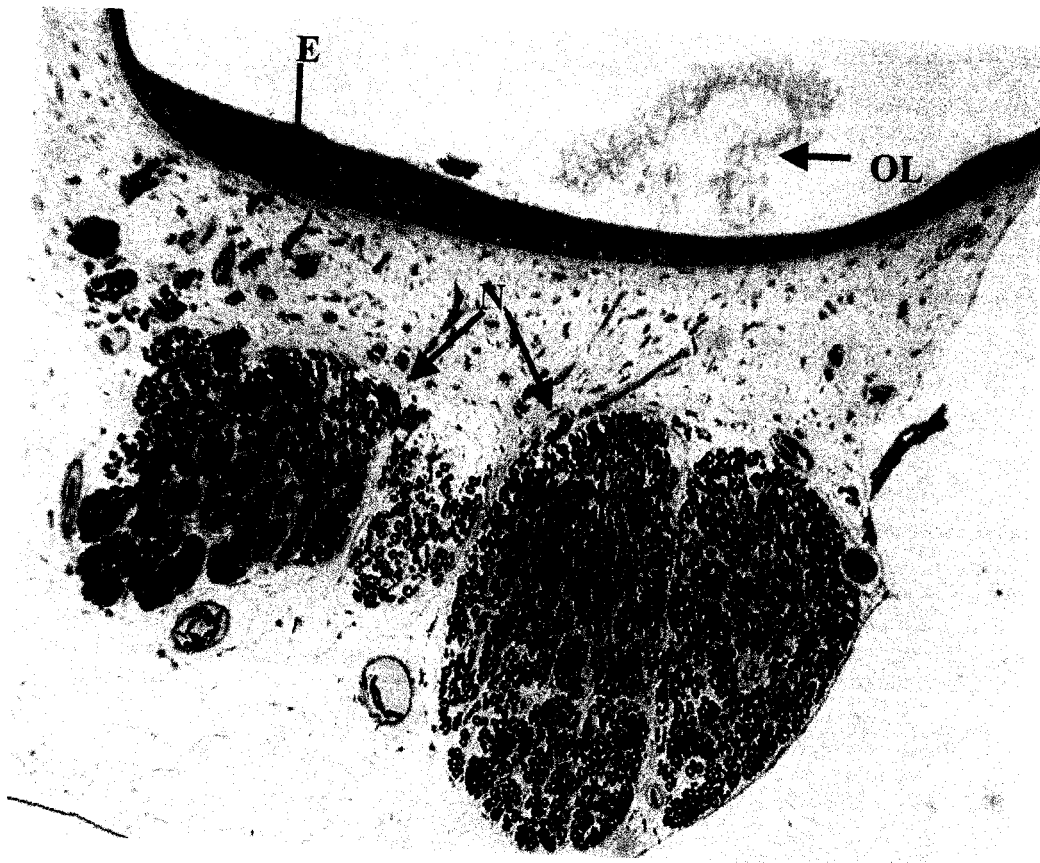


FIGURE 13. LM of a coronal section of the macula and surrounding tissues. The sensory epithelium (E) and anterior branch of the eighth nerve (N) are seen here. Part of the otoconial layer (OL) over the epithelium is also visible in this micrograph. Magnified *ca.* 200x.

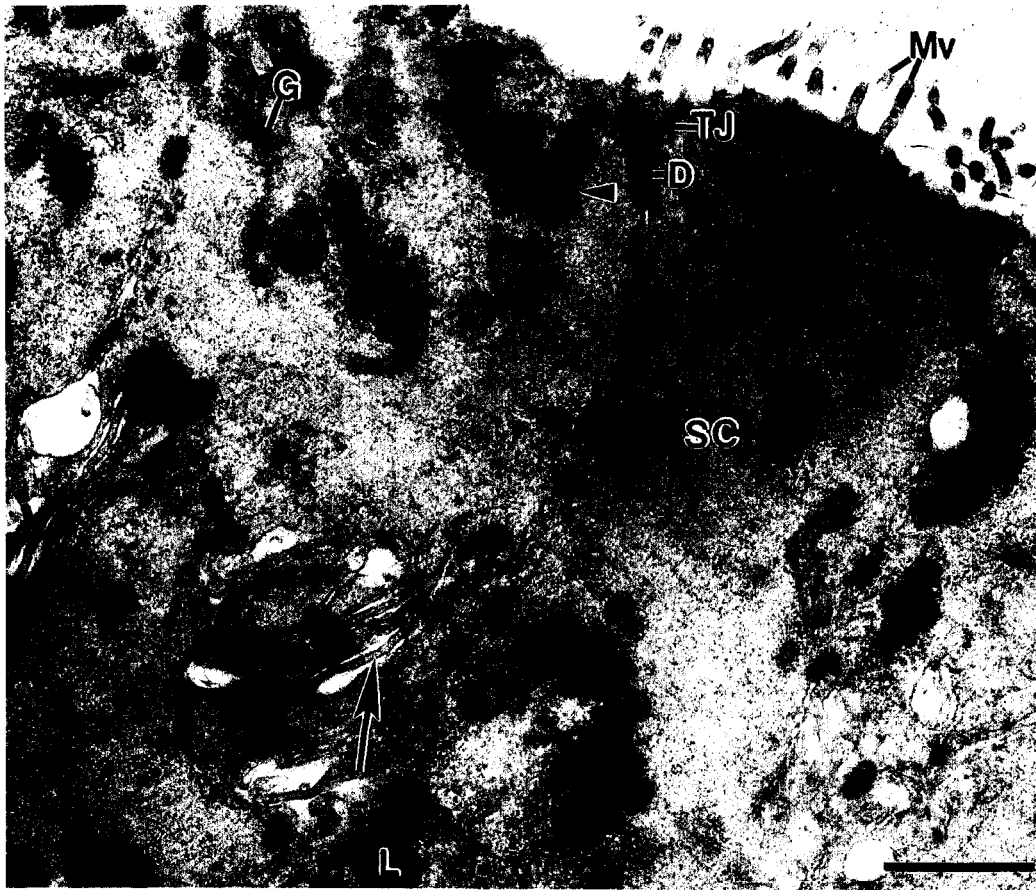


FIGURE 14. TEM of supporting cells (SC). Desmosomes (D) occur along the extensively infolded cell membrane (arrow). The arrowhead indicates an electron-dense granule. Mv: microvilli, TJ: tight junction, G: Golgi complex, L: lysosome. 17,000x. Bar = 1 μ m.

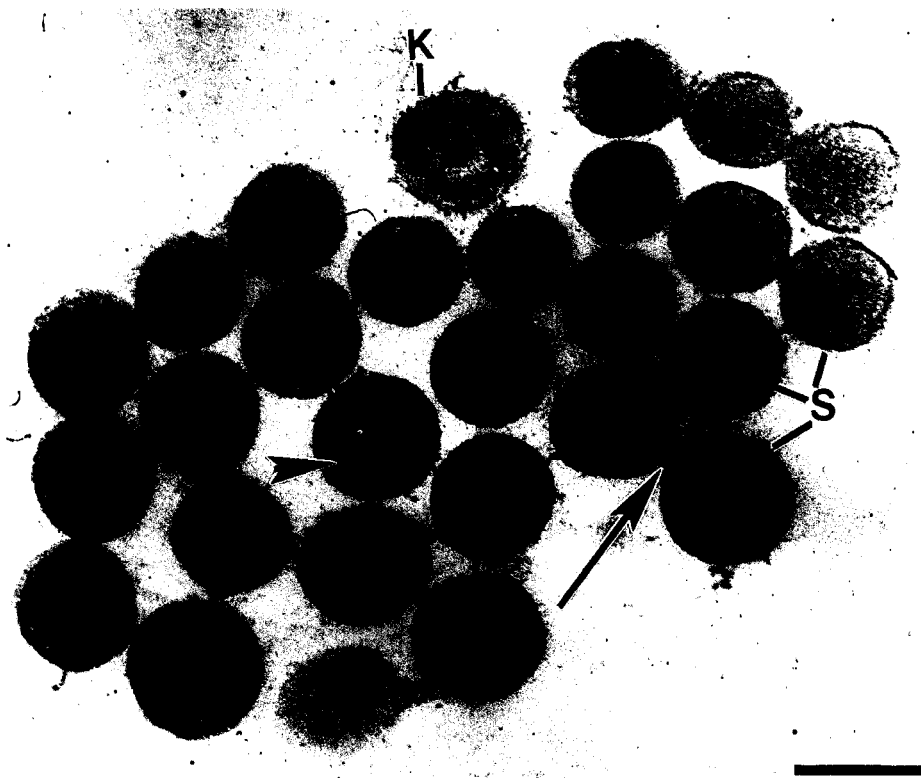


FIGURE 15. TEM of transverse section of a hair bundle. Numerous stereocilia (S) and a single kinocilium (K) are present in this plane of section. Notice the 9+2 arrangement of microtubules in the kinocilium. Stereocilia contain numerous actin filaments (arrowhead) but lack the 9+2 arrangement of microtubules. Interstereociliary connections (arrow) link stereocilia. 56,000x. Bar = 0.25 μ m.

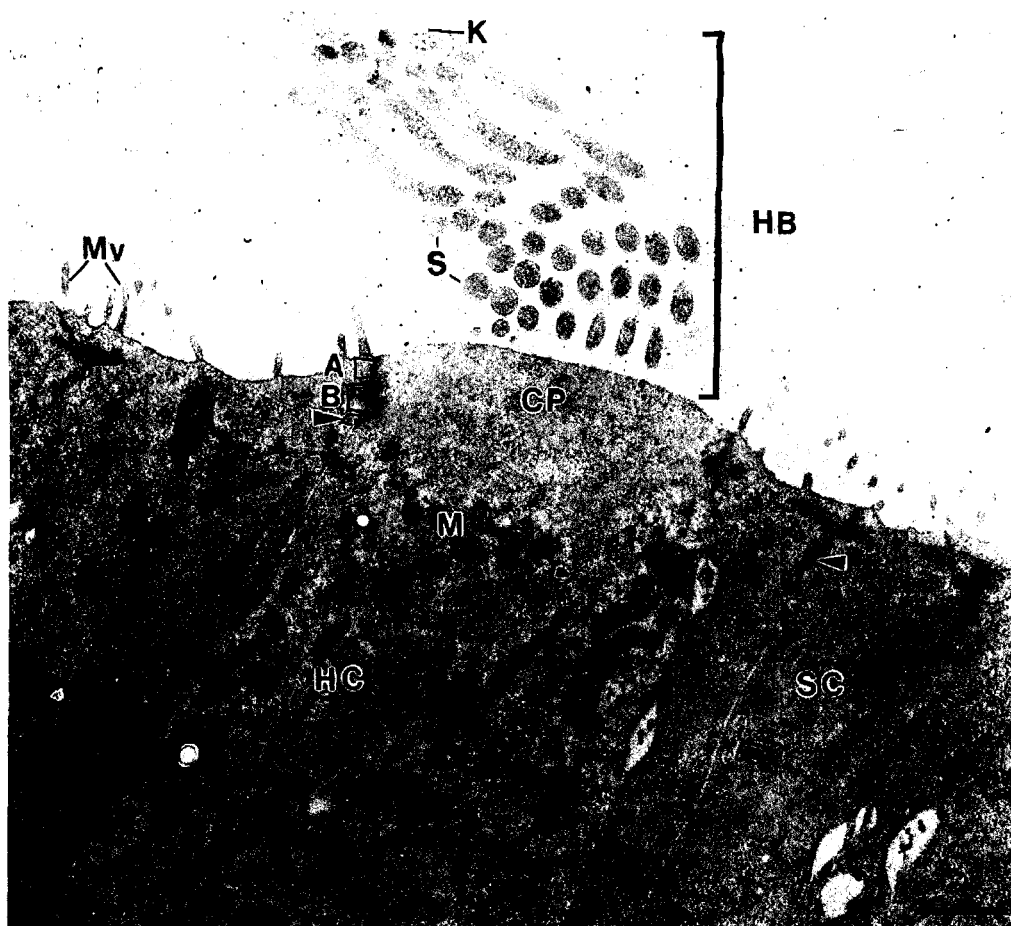


FIGURE 16. TEM of a hair cell (HC) and surrounding supporting cells (SC). The bundle contains numerous stereocilia (S) and a single kinocilium (K). The stereocilia are attached to the cell at the cuticular plate (CP). The cell cytoplasm contains many mitochondria (M), and the cell membrane forms junctional complexes with adjacent supporting cells. A: tight junction, B: macula adherens, Mv: microvilli, arrowheads: desmosomes. 13,300x. Bar = 1 μ m.

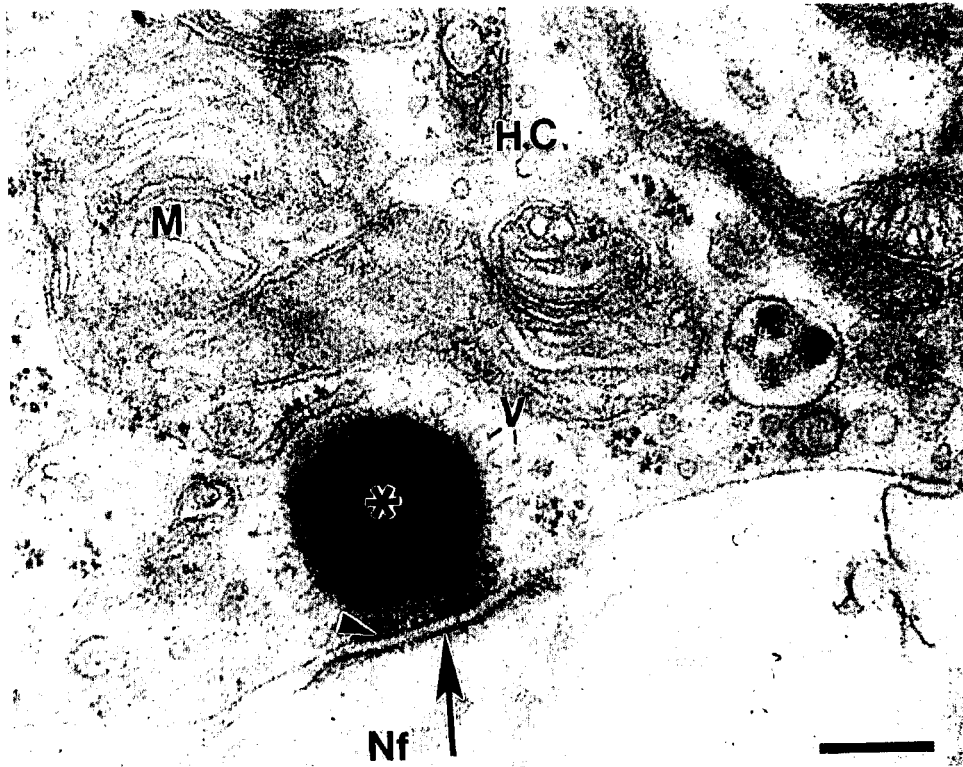


FIGURE 17. TEM of an afferent synaptic body. The micrograph shows a cross-section of an afferent synaptic body in a hair cell (HC). The synaptic body is seen as a dense sphere (asterisk) surrounded by a halo of vesicles (V). The synapse between the hair cell and the afferent nerve fiber (Nf) has a pre-synaptic (arrowhead) and post-synaptic (arrow) thickening. M: mitochondria. 51,000x. Bar= 0.25 μ m.



FIGURE 18. TEM of a cellular process beneath the hair cell (HC). The process is filled with vesicles (V). Mitochondria (M) are also present. In this plane of section, no membrane specializations are apparent. SC: supporting cell. 43,000x. Bar = 0.25 μm .

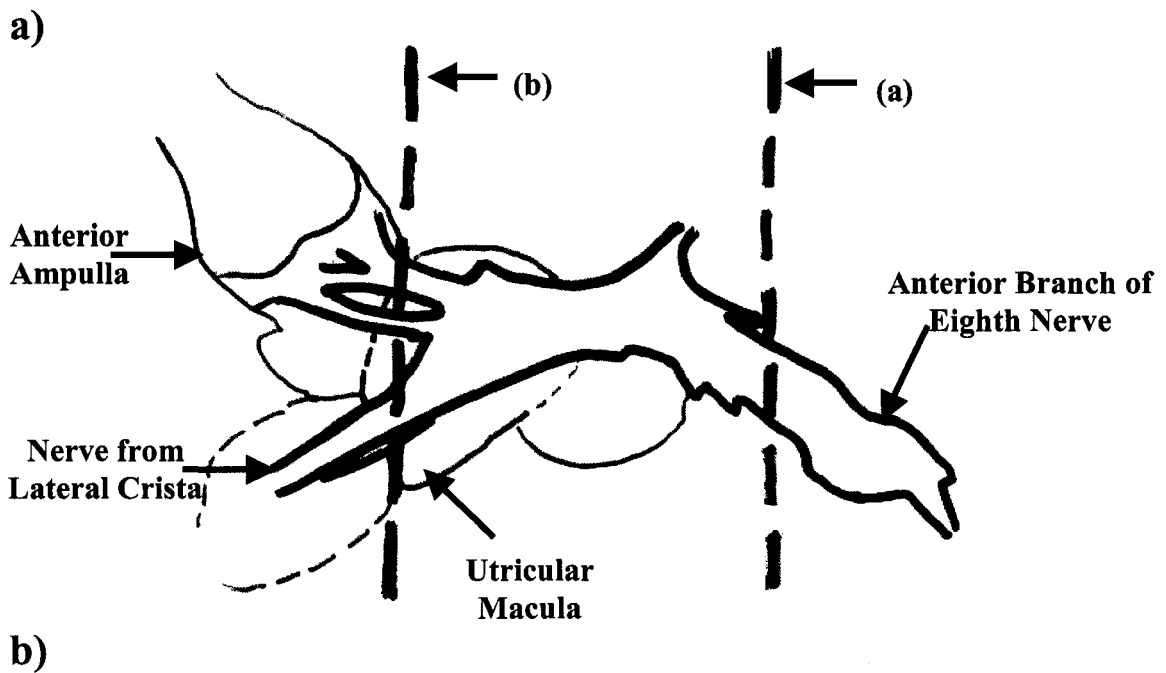


FIGURE 19. LM and tracing of inner ear pars superior. (a) LM of the anterior branch of the eighth nerve. In this specimen, nerves from the anterior and lateral cristae join with those from the utricle to form the anterior branch. In the figure, the specimen has been osmicated and hence the nerve appears black. Magnified *ca.* 6x. (b) Tracing of structures in micrograph. The dashed lines indicate the positions at which montages were made to obtain a count of nerve fibers.



FIGURE 20. LM of the epithelium. On the left is a large neuron in the process of myelination as it exits the epithelium. Terminal branches of most neurons within the epithelium are unmyelinated (arrows). Magnified *ca.* 3,000x.



FIGURE 21. LM of a myelinated fiber within the epithelium. A thin layer of the myelin sheath has been gained by this nerve fiber within the epithelium, a relatively infrequent event. Magnified *ca.* 4,000x.



FIGURE 22. TEM of a nerve fiber (NF) gaining myelin. Numerous folds of the Schwann cell (S) membrane can be seen (arrow) around the nerve fiber. N: nucleus of the Schwann cell, arrowhead: basement membrane, flat arrowhead: neurofilaments. 21,000x. Bar= 0.5 μ m.



FIGURE 23. TEM of myelinated nerve fiber and extracellular material. The micrograph is of a transverse section of the anterior branch showing heavily myelinated axons and extracellular material, collagen fibrils (C). My: myelin sheath, A: axoplasm of the nerve fiber, N: Nucleus of Schwann cell. 14,000x. Bar= 1 μ m.

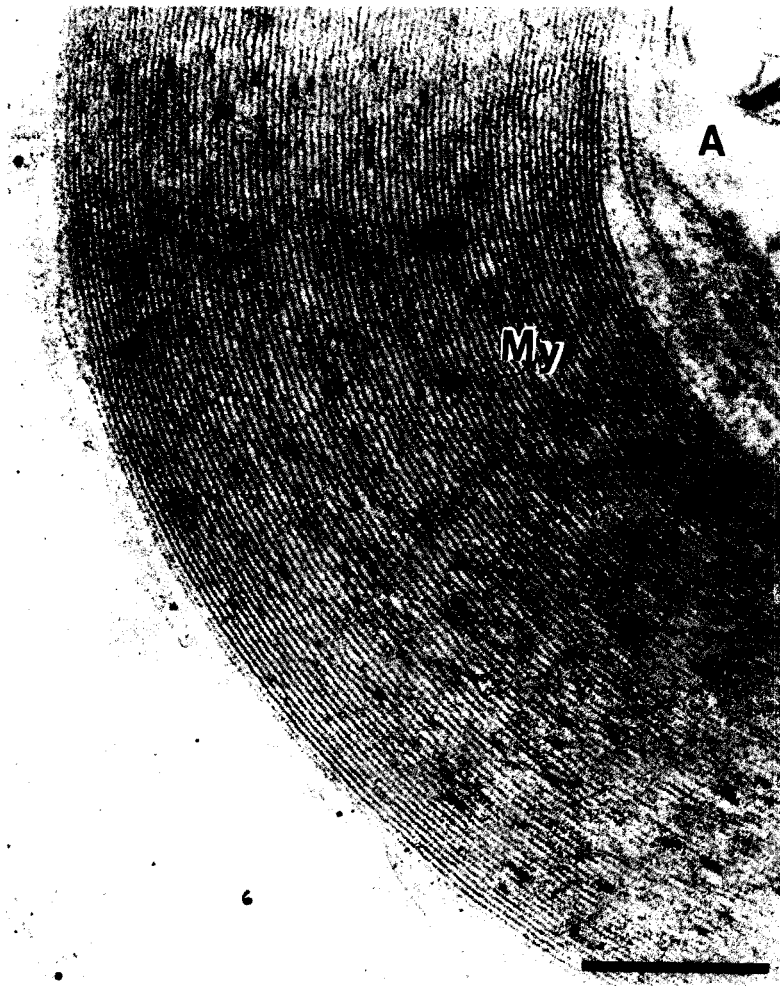


FIGURE 24. TEM of a myelinated axon. There are 73 layers of myelin sheath (My) around this axon. A: axoplasm. 39,000x. Bar = 0.5 μm .

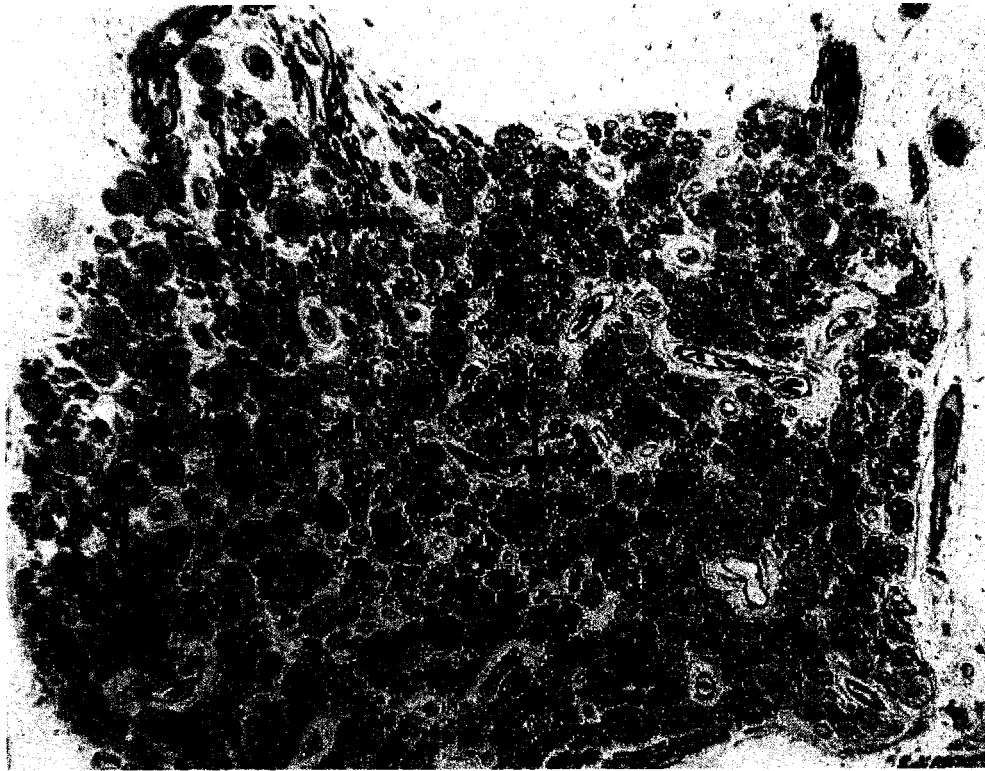


FIGURE 25. LM of the anterior ganglion. Arrows point out the more prominent ganglion cells. Magnified *ca.* 300x.



FIGURE 26. LM of the anterior ganglion cells. Notice the blood vessels (BV) in the section. Arrows: Ganglion cells, R: Red blood cell. Magnified *ca.* 1,200x.

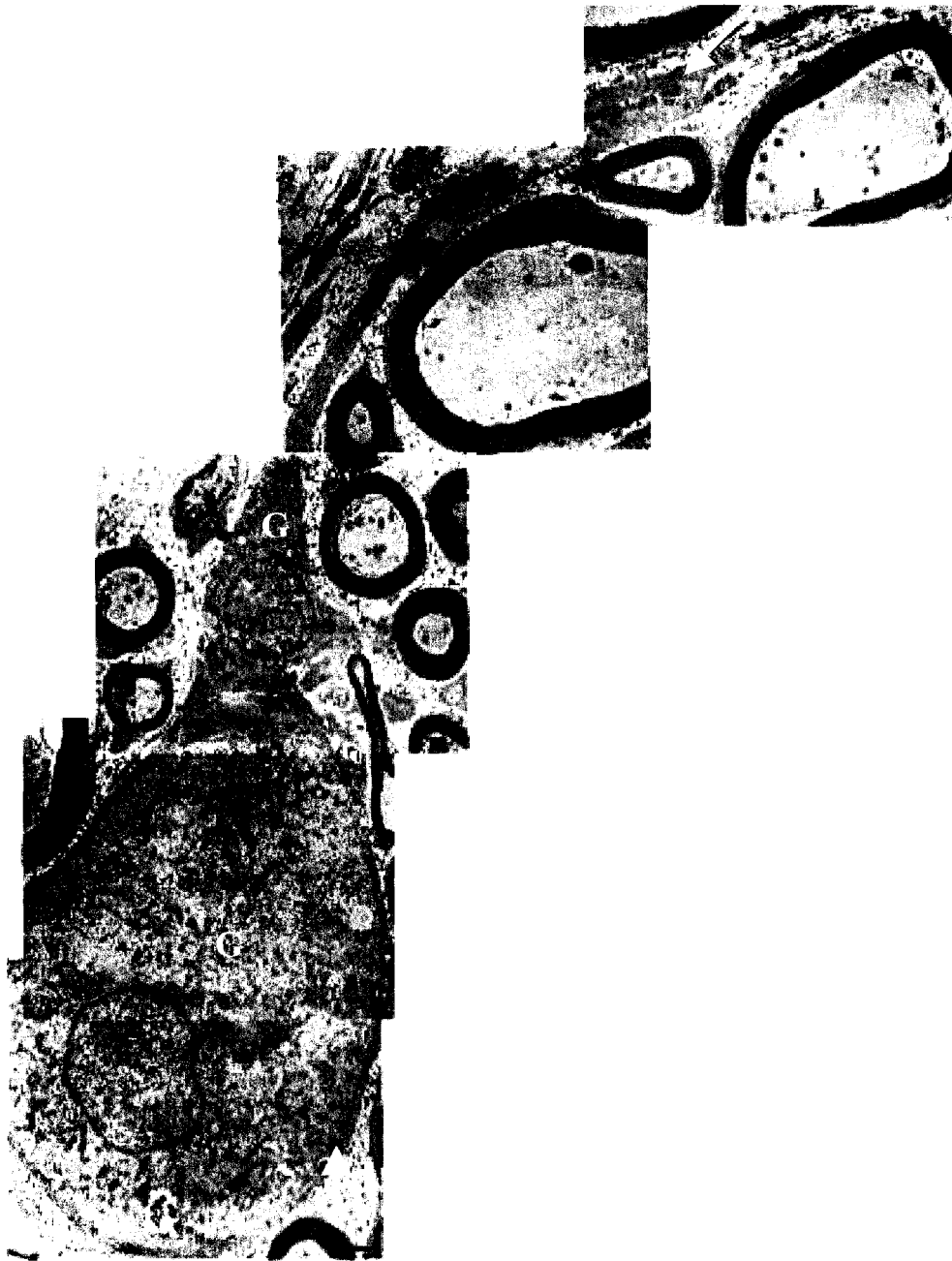


FIGURE 27. TEM montage of two ganglion cells (G). A thin layer of myelin (arrows) can just be seen surrounding the ganglion cell body. 12,000x. Bar =1 μ m.

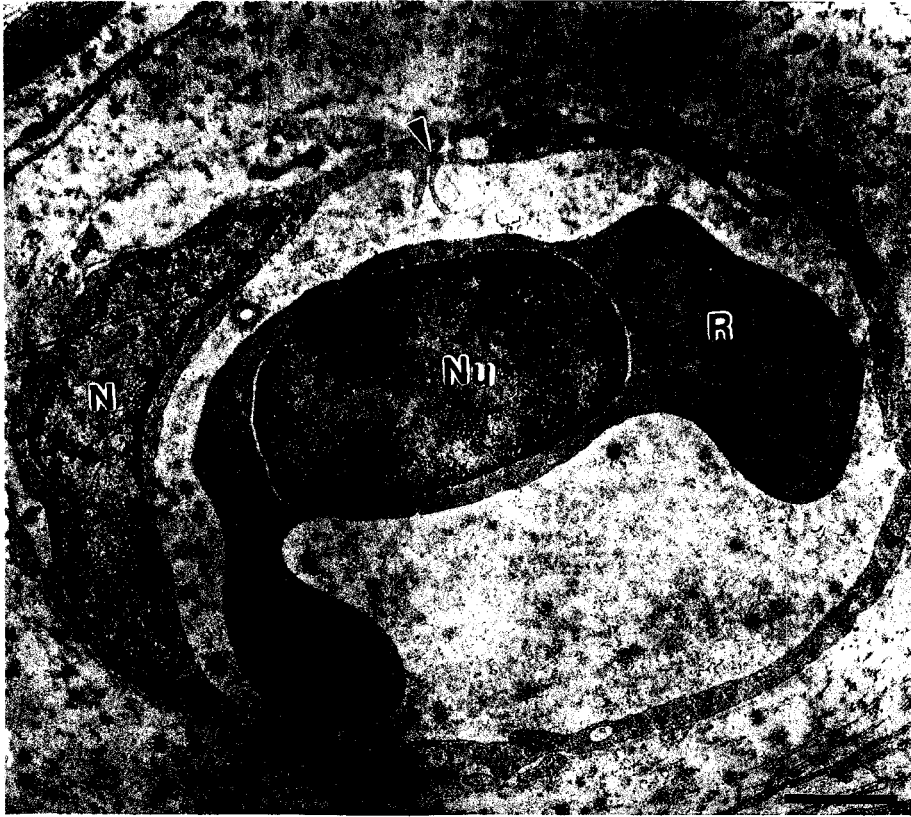


FIGURE 28. TEM of capillary and RBC. The micrograph is of a transverse section of a capillary containing a single nucleated (Nu) red blood cell (R). N: nucleus of an endothelial cell of the capillary epithelium, arrowhead: tight junction. 13,000x. Bar = 1 μ m.



FIGURE 29. TEM of a mast cell. Short pseudopodia (P) extend from its surface. The cytoplasm is filled with characteristically dense granules. Release of a cytoplasmic granule appears to be in progress at the unlabeled arrow. N: nucleus, Nu: nucleolus. 11,000x. Bar = 1 μ m.

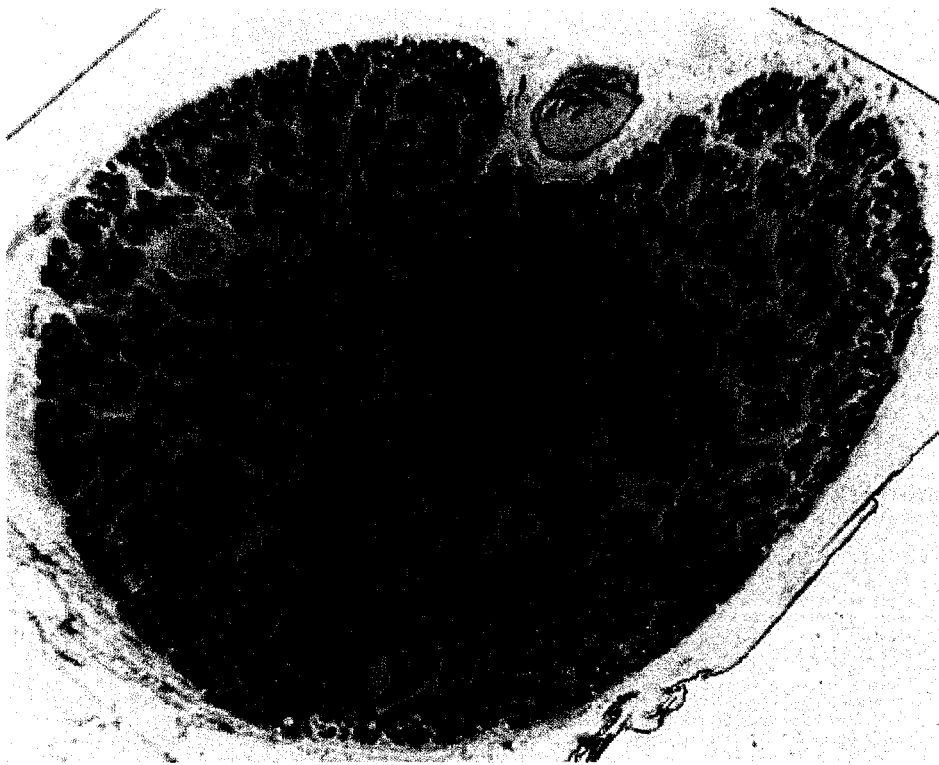


FIGURE 30a. LM of the anterior branch of the eighth nerve. This branch innervates the anterior and lateral cristae as well as the utricle. The section is taken at point (a) in fig.19b. Magnified *ca.* 400x.

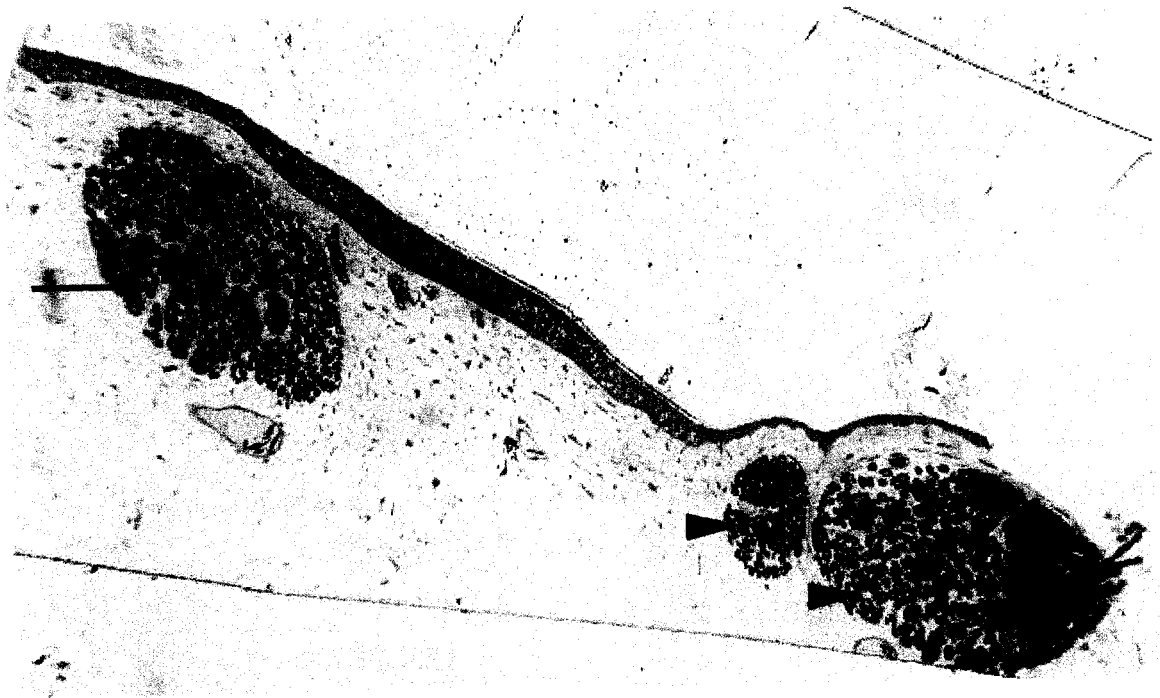


FIGURE 30b. LM of the eighth nerve. The micrograph is taken at point (b) in fig.19b. A single branch (arrow) arises from the lateral crista and two branches (arrowheads) arise from the anterior crista. Magnified *ca.* 400x.

LIST OF TABLES

TABLE 1. Stereocilial counts in hair bundles of different regions of the macula.

Cotillus	Juxtastriola	Striola	Rampa
42	57	51	36
57	59	54	39
64	60	56	40
65		56	52
106		57	58
		58	
		62	
		74	
		84	
		89	

TABLE 2. Comparison of the average number of stereocilia per bundle. The data is from different regions of the macula in three different studies. * does not include the 106 count for one hair cell bundle. (x) indicates the number of bundles counted.

	Cotillus	Juxtastriola	Striola		Rampa
Kothari	57*(4)	59 (3)	65(10)		45 (5)
Severinsen	44		67		38
Moravec	54 (37)		Type I	96 (69)	42 (129)
			Type II	60 (85)	

TABLE 3. Nerve fiber averages from three individual specimens.

	Humans	Bullfrogs	Turtle (N = 3)
Before Branching			2,814
Lateral Crista	1,480		744
Anterior Crista	1,338		808
Utricular Macula	3,023	2,315	1,263
NF/HC	1:10		1:8

TABLE 4. Average diameters of nerve fibers. 27 nerve fibers were measured at random locations in 3 separate anterior branch locations.

Sample	1	2	3	Average
Large Fibers (μm)	4.99 6.66 6.66	8.33 8.33 11.66	6.66 6.66 6.66	7.4
Medium Fibers (μm)	2.49 2.49 3.33	4.99 6.66 6.66	3.33 4.16 4.99	5.1
Small Fibers (μm)	4.16 4.99 5.28	2.5 3.33 3.33	2.5 2.5 2.5	2.8

APPENDIX 2: SOLUTION FORMULATIONS

1. Fixative

Paraformaldehyde	2%
Glutaraldehyde	3%
Sodium Cacodylate Buffer	0.1 M
Acrolein	1%

- The paraformaldehyde was added to the sodium cacodylate buffer and left on the stirrer overnight (till the paraformaldehyde dissolved).
- Next the glutaraldehyde and acrolein were added just prior to use.
- The fixative was refrigerated when not in use.

2. Decalcification Solution

Glutaraldehyde	2%
EDTA (ethylenediametetraacetic acid)	0.1 M
Sodium Cacodylate Buffer	0.1 M

- The three solutions were mixed and stirred.
- This solution was always prepared fresh just prior to use.

3. Osmium Tetroxide

0.25 g in 25 ml 0.1 M Sodium Cacodylate buffer.

- 12.5 ml 0.2M sodium cacodylate buffer + 12.5ml deionized (DI) water.
- The osmium tetroxide vial was broken and put in a flask containing the buffer in DI water.
- Sodium cacodylate was introduced in the vial with the help of a pipette.
- The flask was then covered with parafilm and stirred. When in solution, the parafilm turned black.

4. Resin

A one-step single formula mix for a soft block was used.

Embed 812	20 ml
DDSA	22 ml
NMA	5 ml
DMP-30	0.70 ml

- Immediately before use, the Embed 812, DDSA (Dodecenyl Succinic Anhydride), and the NMA (Nadic Methyl Anhydride) were mixed in a flask on a stirrer.

- Next the DMP-30 (2,4,6-Tri(dimethylaminomethyl) phenol) (accelerator) was added followed by thorough mixing on the stirrer.
- The prepared mixture (without the accelerator) can be stored for up to 6 months at 4 °C. However, it is recommended that freshly prepared embedding medium be used.
- If storing the mixture, it should be warmed before adding the accelerator prior to use.

5. Toluidine Blue (100 ml)

Toluidine Blue	1g
Sodium tetraborate	1 g
Deionized Water	100 ml

Kept on stirrer for 1 hour (or till toluidine blue dissolved). Filtered prior to use.

6. 2% Uranyl Acetate

Prepared 15-50 ml aqueous uranyl acetate. A minimum of 60 minutes with constant agitation on a magnetic stirrer was required to dissolve the crystals. It was then filtered to remove any undissolved crystals.

7. Reynold's Lead Citrate

Lead Nitrate	1.33 g
Sodium citrate	1.76 g
1N Sodium hydroxide	8.0 ml
Glass distilled water	~100ml

- Dissolved 1.33 g lead nitrate in 30 ml boiled (then cooled), glass distilled (or Millipore filtered) water in a 50 ml volumetric flask.
- Added 1.76 g sodium citrate. Sealed the flask tightly with two layers of parafilm and shook it for 1 minute. It was then kept aside for 30 minutes with intermittent shaking.
- Added 8.0ml 1N sodium hydroxide.
- Diluted to 50 ml with boiled, then cooled, glass-distilled water, and mixed by inversion several times. If the solution remained turbid, it was centrifuged it before use. The flask was covered with aluminum foil, resealed with parafilm, the container (including date) labeled, and refrigerated.